

Intraseasonal, interannual and seasonal variability of
zooplankton biomass and standing stock inferred from ADCP
backscatter in the eastern Arabian Sea

Ranjan Kumar Sahu^{1,2}, D. Shankar^{1,2}, P. Amol^{2,3}, S.G.Aparna^{1,2}, and D.V. Desai^{1,2}

¹CSIR-National Institute of Oceanography, Dona Paula, 403004, Goa, India.

²Academy of Scientific and Innovative Research (AcSIR), Ghaziabad, 201002,
Uttar Pradesh, India.

³CSIR-National Institute of Oceanography, Regional Centre, 530017,
Visakhapatnam, India.

December 31, 2024

¹ **Abstract**

The spatio-temporal variation of zooplankton biomass and standing stock in the eastern Arabian Sea (EAS) is mapped using backscatter measurements from 153.3 kHz acoustic Doppler current profiler (ADCP) moorings deployed at seven locations on the continental slope off the west coast of India from October 2017 to December 2023. The conversion from backscatter to biomass is

6 based on volumetric zooplankton sampling at the respective locations. Analysis of the data over
7 24–140 m shows that the backscatter and zooplankton biomass decrease from the upper ocean
8 ($215/175 \text{ mg}^{-3}$ biomass contour) to the lower depths. Changes are observed in the seasonal variation
9 of the monthly climatology of zooplankton standing stock (integral of the biomass over 24–120
10 m water column) as we move to poleward along the slope in EAS. The range of variation of
11 standing stock is lowest at Kanyakumari, followed by Okha, which lie at the southern and northern
12 boundary of the EAS, respectively. While annual cycle is predominant at northeastern Arabian
13 Sea (NEAS), it decreases towards southeastern Arabian Sea (SEAS) where the semi-annual cycle
14 tends to dominate. Analysis reveals weak presence of annual cycle in zooplankton biomass and it
15 is dominated by intraseasonal and intra-annual components. Strong interannual variability, which
16 is rarely addressed in conventional studies, is observed off Kollam with peaks corresponding to
17 period of ~ 720 days, moderately off Mumbai and feebly off Goa. Intraseasonal variability is often
18 comparable (stronger) to the intra-annual (annual) variability both of which increases (decreases)
19 poleward with an evident presence in SEAS. Stronger intraseasonal variability has implication on
20 zooplankton sampling using conventional methods and its patchiness in open ocean. Further, it
21 also impacts the accurate estimation of standing stock and on reduced predictability of biomass.

22 **1 Introduction**

23 **1.1 Background**

24 Zooplankton plays a vital role in food web of pelagic ecosystem by enabling the hierarchical trans-
25 port of organic matter from primary producers to higher trophic levels impacting the fish population
26 [Ohman and Hirche, 2001] and the carbon pump of the deep ocean [Quéré et al., 2016]. They are
27 presumably the largest migrating organisms in terms of biomass [Hays, 2003] which occurs in diel
28 vertical migration (DVM). Zooplankton depend not only on phytoplankton but other environmental
29 parameters (e.g. mixed-layer depth, insolation, oxygen, thermocline, nutrient availability, chl-a con-
30 centration and daily primary production). The biological productivity of the ocean is essentially
31 connected with physics and chemistry [Subrahmanyam, 1959, Ryther et al., 1966, Qasim, 1977,
32 Nair, 1970, Banse, 1995, McCreary et al., 2009, Vijith et al., 2016, Amol et al., 2020]. The dynamic
33 ocean results in varying physico-chemical properties, leading to bloom and growth of plankton in
34 favourable conditions. The changes are strongly influenced by the seasonal cycle in the North
35 Indian Ocean (NIO; north of 5 °N of Indian Ocean). The eastern boundary of Arabian Sea con-
36 tains the West India Coastal Current [WICC; Ramamirtham and Murty, 1965, Banse, 1968, Shetye
37 et al., 1990, McCreary et al., 1993, Amol et al., 2014, Vijith et al., 2016, Chaudhuri et al., 2020]
38 which reverses seasonally, flowing poleward (equatorward) during November to February (June to
39 September) [Shetye et al., 1990, 1991, Vijith et al., 2022].

40 A direct consequence of this reversal is the seasonal cycle of thermocline [Prasad and Bahulayan,
41 1996, Kumar and Narvekar, 2005], oxycline [DeSousa et al., 1996, Schmidt et al., 2020] and thickness
42 of mixed-layer depth [MLD; Shetye et al., 1991, Prasad and Bahulayan, 1996, Kumar and Narvekar,
43 2005] induced by upwelling (downwelling) favourable conditions in summer (winter) at eastern

44 Arabian Sea (EAS) facilitated further by wind speed and near-surface stratification. Further, the
45 phytoplankton biomass and chl-a concentration changes with the season [Subrahmanyam and Sarma,
46 1960, Banse, 1968, Kumar and Narvekar, 2005, Lévy et al., 2007, Vijith et al., 2016]. Upwelling
47 in summer monsoon leads to maximum chl-a growth in the entire EAS [Banse, 1968, Banse and
48 English, 2000, McCreary et al., 2009, Hood et al., 2017, Bemal et al., 2018, Shi and Wang, 2022].
49 During winter monsoon, the convective mixing induced winter mixed layer [Shetye et al., 1992,
50 Madhupratap et al., 1996b, McCreary et al., 1996, Lévy et al., 2007, Shankar et al., 2016, Vijith
51 et al., 2016, Keerthi et al., 2017, Shi and Wang, 2022] results in winter chl-a peak at NEAS while
52 the downwelling Rossby waves modulate chl-a along SEAS albeit limited to coast and islands [Amol
53 et al., 2020].

54 The zooplankton grazing peak is instantaneous with no time delay from peak phytoplankton
55 production [Li et al., 2000, Barber et al., 2001], but its population growth lags [Rehim and Imran,
56 2012, Almén and Tamelander, 2020] depending on its gestation period and other limiting aspects.
57 While some studies suggest that the peak timing of zooplankton may not change in parallel with
58 phytoplankton blooms [Winder and Schindler, 2004], others indicate that lag exists between primary
59 production and the transfer of energy to higher trophic levels [Brock and McClain, 1992, Brock
60 et al., 1991]. The conventional zooplankton measurements, where only few snapshot/s of the event
61 is captured gives an incoherent or incomplete understanding in terms of spatio-temporal variation
62 of zooplankton [Ramamurthy, 1965, Pionkovski et al., 1995, Madhupratap et al., 1992, 1996a,
63 Wishner et al., 1998, Kidwai and Amjad, 2000, Barber et al., 2001, Khandagale et al., 2022] as
64 much information is revealed by later studies [Jyothibabu et al., 2010, Shankar et al., 2019, Aparna
65 et al., 2022] using high resolution data. Calibrated acoustic instruments such as acoustic Doppler
66 current profiler (ADCP) along with relevant data can be utilised to understand small scale variability

67 [Nair et al., 1999, Edvardsen et al., 2003, Smith and Madhupratap, 2005, Smeti et al., 2015, Kang
68 et al., 2024], the complex interplay between the physico-chemical parameters and ecosystem [Jiang
69 et al., 2007, Potiris et al., 2018, Shankar et al., 2019, Aparna et al., 2022, Nie et al., 2023], the
70 zooplankton migration [Inoue et al., 2016, Ursella et al., 2018, 2021] and their seasonal to annual
71 variation [Jiang et al., 2007, Hobbs et al., 2021, Liu et al., 2022, Aparna et al., 2022].

72 The relationship between backscatter and the abundance and size of zooplankton was described
73 by Greenlaw [1979] wherein it was pointed out that single frequency backscatter can be used to esti-
74 mate abundance if mean zooplankton size is known. A drastic increase in study temporal and spatial
75 variation of zooplankton biomass using backscatter-proxy came in 1990s by introduction of high-
76 frequency echo sounders, with studies [Flagg and Smith, 1989, Wiebe et al., 1990, Batchelder et al.,
77 1995, Greene et al., 1998, Rippeth and Simpson, 1998] methodically showing acoustic backscatter
78 estimated zooplankton biomass. Net sampling augmented ADCP backscatter have been used to
79 study DVM and the spatial and temporal variability of zooplankton biomass in different marine
80 regions, such as the Southwestern Pacific, the Lazarev Sea in Antarctica and the Corsica Channel
81 in the north-western Mediterranean Sea [Cisewski et al., 2010, Hamilton et al., 2013, Smeti et al.,
82 2015, Guerra et al., 2019]. The first such study to exploit the potential of ADCPs in EAS was
83 carried out by Aparna et al. [2022] (A22 from hereon) using ADCP moorings deployed on conti-
84 nental slopes off the Indian west coast. In their work, they showed that the zooplankton standing
85 stock (ZSS) in fact declines during upwelling facilitated increase in phytoplankton biomass. The
86 unusual interaction implies the break down of existing understanding of predator-prey relationship
87 in fundamental level of marine food chain.

88 **1.2 Objective and scope of the manuscript**

89 A network of ADCPs has been installed off the continental slope and shelf on the west coast of
90 India. This ADCPs have enabled a rigorous view of intraseasonal to seasonal scale variability [[Amol](#)
91 [et al., 2014](#), [Chaudhuri et al., 2020](#)] of WICC. In the recent study A22 have used ADCP moorings
92 off Mumbai, Goa and Kollam to explain the temporal variability of zooplankton biomass. The
93 study showed that the zooplankton peaks (and troughs) is not only non-uniform in latitude but
94 also heavily influenced by the oxygen minimum zone, MLD and the seasonal upwelling/downwelling
95 conditions. Stark contrast in the phytoplankton bloom and subsequence growth of zooplankton or
96 the lack thereof was observed in the EAS regimes.

97 We extend the work of A22 by presenting data from four additional moorings in the EAS, show-
98 casing the deviations of seasonal cycle from climatology, and discussing the significant intraseasonal
99 variability of biomass and standing stock revealed by the ADCP data. The paper is organized as
100 follows; datasets and methods employed are described in section 2. Section 3 describes the observed
101 climatology of zooplankton biomass and standing stock. A comparison is drawn to the results of
102 A22. Further, the seasonal cycle of zooplankton biomass and standing stock is discussed with re-
103 lation to the MLD, oxygen, temperature and circulation in determining the biomass is discussed
104 in results section 4. Section 5 delves deeper into the intraseasonal variability with summary and
105 conclusion in section 6.

106 **2 Data and methods**

107 The backscatter data from ADCP and the zooplankton samples collected from the periphery of
108 mooring is described in this section. The backscatter derived from the echo intensity of the seven

109 ADCP mooring deployed on the continental slope off the Indian west coast is the primary data we
110 have use in this manuscript. The moorings details are summarized in [table 1](#). In situ biomass data
111 from volumetric zooplankton samples are used to validate and correlate with backscatter. The chl-a
112 data is used to study and draw inferences for the possible zooplankton growth seasons. In addition,
113 we have used the monthly climatology of temperature and salinity from [Chatterjee et al. \[2012\]](#).

114 2.1 ADCP data and backscatter estimation

115 The ADCPs were deployed on the continental slope off the Indian west coast ([Fig. 1](#)), off Mumbai,
116 Goa, Kollam and Kanyakumari, and later extended to three more sites to cover the entire EAS
117 basin from Okha (22.26°N) in north to Kanyakumari (6.96°N) in south. The other two ADCPs
118 are, 1) Jaigarh at central EAS (CEAS), 2) Udupi (primarily at SEAS regime) in the transition
119 zone between CEAS and SEAS. The extended moorings were deployed in October 2017, though
120 Kanyakumari had been deployed earlier too. However, only Mumbai, Goa and Kollam were part of
121 the previous backscatter study by A22. The moorings are serviced on yearly basis usually during
122 October–November or sometime during September–December (depending on ship availability). The
123 ADCPs are of Teledyne RD Instruments make, upward-looking and operate at 153.3 kHz. While
124 utmost care is taken to position the instrument (mooring) at \sim 150–200 m (\sim 1050–1100 m) depth,
125 yet for some deployments it's shallow or deeper owing to drift caused by floater buoyancy-anchor
126 weight balance. Data was collected at hourly interval and the bin size was set to 4 m. The echoes at
127 surface to 10% range (\sim 20 m) means the data at these depths is rendered useless and is discarded
128 from further use. We have followed the methodology laid down in A22 to derive the backscatter
129 time series from ADCP echo intensity data. The gaps up to two days are filled using the grafting
130 method of [Mukhopadhyay et al. \[2017\]](#) once the zooplankton biomass time series is constructed.

131 **2.2 Zooplankton data and estimation of biomass**

132 The zooplankton samples were collected in the vicinity (~ 10 km) of ADCP mooring site twice,
133 once prior retrieval and again post deployment of moorings so that there is overlap in the ADCP
134 time instance and in situ zooplankton samples during servicing cruises on board of RV Sindhu
135 Sankalp and RV Sindhu Sadhana ([table 2](#)). Multi-plankton net (MPN) (100 μm mesh size, 0.5 m^2
136 mouth area) was used to get samples in the pre-determined depth ranges; water volume filtered was
137 calculated by the product of sampling depth range and the mouth area of net. The depth range
138 and timing of sample collection was different throughout the MPN hauls (refer [table 2](#)). From 2020
139 onward, the depth-range was standardized to the bins of 0–25, 25–50, 50–75, 75–100, 100–150 (units
140 are in meters). The backscatter obtained earlier is averaged in vertical corresponding to the specific
141 MPN hauls for each site. The backscatter is linearly regressed with respective biomass to establish
142 their relationship ([Fig. 2](#)), which has been demonstrated in numerous previous studies [[Flagg and](#)
143 [Smith, 1989](#), [Heywood et al., 1991](#), [Jiang et al., 2007](#), [Aparna et al., 2022](#)].

144 **2.2.1 Biomass time series and estimation of standing stock**

145 The zooplankton biomass time series ([Fig. 3](#)) is created from the above derived linear relationship.
146 The standing stock is determined by taking the depth integral of biomass over the water column.
147 To maintain the consistency of standing stock estimation, only those deployments that doesn't lack
148 data at any depth in the entire range of 24–120 m are considered for analysis as in A22. The lack of
149 data in the above mentioned depth range is due to deviation in positioning of ADCP sensor in the
150 water column. A swift alteration in bathymetry along the continental slope implies that the mooring
151 might anchor at a different depth than planned, hence a change in the predicted position of ADCP.
152 This leads to gap in data at few mooring sites for some year. For example, for the northern-most

153 mooring at Okha, data is not available for the entire upper 120 m depth for the second deployment.
154 Also at Jaigarh, where the surface to ~60 m data (in 3rd deployment) and Kollam, where 80 m
155 and below (in 4th deployment) is unavailable and hence discarded from standing stock estimation.
156 There are few deployments where no or bad data was recorded e.g, at Udupi (4th deployment) and
157 Kanyakumari (6th deployment).

158 **2.3 Mixed-layer depth, temperature, oxygen and chlorophyll**

159 As we are using a 153.3 kHz ADCP moored at ~150 m, the top ~10% of data is unusable because
160 of surface echoes. MLD in EAS is of the order ~20 to 40 m during summer monsoon [Shetye et al.,
161 1990, Shankar et al., 2005, Sreenivas et al., 2008] especially in the SEAS [Shenoi et al., 2005], but
162 during winter the MLD in northern NEAS remains deep [Shankar et al., 2016]. The temperature
163 data is used from Chatterjee et al. [2012], a monthly climatology having 1° spatial resolution.
164 Monthly climatology of oxygen data is obtained from World Ocean Atlas 2013 [García et al., 2014]
165 which contains objectively analyzed 1° climatological fields of in situ measurements. Previous
166 study based on ADCP data of EAS A22 have used SeaWiFS based chl-a data for comparison with
167 climatology of ZSS. The SeaWiFS was at its end of service in 2010, hence we use new chl-a product
168 from Global Ocean Colour, biogeochemical L3 data obtained from [E.U. Copernicus Marine Service](#)
169 [Information](#). The daily data is available at a spatial resolution of 4 km.

170 **3 Time series, climatology and seasonal cycle**

171 A decrease in biomass with increasing depth at all seven study sites is observed ([Fig. 3](#)). To
172 distinguish between high and low productivity zones, we employed a biomass contour, similar to the
173 215 mg m⁻³ threshold used in A22. However, to better capture seasonal variations off Kanyakumari

¹⁷⁴ and Okha, the threshold was replaced by 175 mg m^{-3} . The biomass contour z215 (depth contour
¹⁷⁵ D215) and z175 (depth contour D175) allows us to link the seasonal variation of biomass to the
¹⁷⁶ physico-chemical properties. The monthly climatology of biomass and ZSS is computed for all
¹⁷⁷ locations having valid data in 24–140 m depth range. Climatology of zooplankton biomass and
¹⁷⁸ ZSS is discussed at locations northward starting from southernmost mooring site i.e, Kanyakumari.
¹⁷⁹ Time series, climatology and seasonal cycle of biomass is discussed in the following [section 3.2](#). For
¹⁸⁰ a comparison with physico-chemical forcing similar to A22, we use isotherm of 23°C (henceforth,
¹⁸¹ D23) and oxygen contour specific to each site depending on its position relative to oxygen minimum
¹⁸² zone (OMZ) boundaries of EAS.

¹⁸³ 3.1 Time series description

¹⁸⁴ Rate of biomass decrease with depth, roughly defined as the difference between mean biomass at 40
¹⁸⁵ and 104 m depth is highest off Jaigarh and Mumbai as it has higher biomass in upper ocean ([Fig. 4](#))
¹⁸⁶ and lowest off Kanyakumari. This is followed by Goa and Udupi. While the biomass decrease with
¹⁸⁷ depth is lower off Kollam from 2017 to 2020, it becomes considerably high from thereon ([Fig. 4 f](#)).
¹⁸⁸ A comparatively moderate decline in zooplankton biomass with respect to depth off Okha ([Fig. 3](#)
¹⁸⁹ a1, a2) at NEAS is agreeing with earlier reported data [[Wishner et al., 1998](#), [Madhupratap et al.,
2001](#), [Smith and Madhupratap, 2005](#), [Jyothibabu et al., 2010](#)]. The difference of mean biomass at 40
¹⁹⁰ and 104 m is high at most location but it arises due to the bigger difference in select few years, e.g.,
¹⁹¹ off Mumbai during 2020 and 2022, off Jaigarh in 2021, at Goa during 2021–2022, off Kollam during
¹⁹² 2022. The sites at SEAS, particularly off Kanyakumari for all years and 2017 to 2020 off Kollam
¹⁹³ also have weaker decrease [[Madhupratap et al., 2001](#), [Jyothibabu et al., 2010](#), [Aparna et al., 2022](#)].
¹⁹⁴ However, the biomass decline with depth post 2021 off Kollam is high owing to a strong bloom in
¹⁹⁵

¹⁹⁶ these years and is reflected as D215 deepening. D175 and D215 is deep throughout EAS during
¹⁹⁷ winter monsoon as seen from the same biomass value at 40 and 104 m indicating the penetration
¹⁹⁸ of D215/D175 all the way to 104 m, but the occurrence of high biomass is distinct to each regime
¹⁹⁹ of EAS. Upper ocean shows considerably high biomass and ZSS during winter monsoon at NEAS.
²⁰⁰ On the contrary at SEAS, the upper ocean shows higher biomass during summer monsoon even
²⁰¹ though the D215 and D175 is shallower during this period.

²⁰² Variation in the monthly average or seasonal cycle over time suggests presence interannual
²⁰³ variability. Consider the case of Kollam, for the years 2019 and 2020 the low biomass is observed at
²⁰⁴ depths as much as near to the surface regime resulting in shallower D215. But for the years 2018,
²⁰⁵ 2022, and 2023 the high biomass occurs at deeper depths too leading to a much deeper D215. Since
²⁰⁶ we can't use two contours for demarcating the high biomass for same time series, we have refrained
²⁰⁷ from using the D215 for the year 2020 when it is shallowest and isn't a representative of the seasonal
²⁰⁸ variation. The mean, standard deviation of biomass, ZSS and chl-a are shown in supplementary
²⁰⁹ table S1. There is no consistent variation as seen from the analysis of mean and standard deviation
²¹⁰ of biomass at 40 and 104 m. The sites with higher biomass tends to have higher variation over time
²¹¹ e.g. Mumbai, Jaigarh and Kollam. Superposed on the time-series is seasonal cycle and variability
²¹² of distinct period band, a detailed discussion on this is presented in [section 3.3](#).

²¹³ 3.2 Climatology of zooplankton biomass and standing stock

²¹⁴ Off Kanyakumari, z175 is shallower from May onward till October and the zooplankton biomass
²¹⁵ is comparatively higher than rest of the year ([Fig. 5 g1](#)). The D23 isotherm along-with oxycline
²¹⁶ (marked by 2.1 ml L^{-1} , a higher oxygen contour as it lies outside OMZ core) follows the same
²¹⁷ seasonal cycle like D175. However, there is almost no seasonal variation in ZSS off Kanyakumari

(σ , 0.67 gm m^{-2}) as compared to the chl-a variation (σ , 1.53 mg m^{-3}). At the nearest northern mooring site off Kollam, a strong seasonal cycle is observed and the D215 is deeper for any given month. A decline (steep-rise) in ZSS (chl-a biomass) is seen and its minimum (peak) is attained in August (Fig. 5 f2). This feature was previously reported by A22, highlighting an imbalance in the interaction between zooplankton and phytoplankton, it occurs due to shallowing of thermocline and low oxygen, and that's why the ZSS is at it's minimum when chl-a peaks. A similar feature is seen further north, off Udupi which sits at the transition zone of SEAS and CEAS, albeit with a relatively weaker zooplankton biomass and minimum (peak) of ZSS (chl-a) occurring a month later during September.

The D215 seasonal trend off Goa in present study is similar to trend of D215 off Goa as described in A22 (See section S1 for comparison). The biomass off Goa decreases rapidly below the z215 as reported earlier, reaching as low as 60 mg m^{-3} at 130 m during June to September (Fig. 5 d1). The ZSS off Jaigarh is identical but stronger to that of off Goa, owing to higher biomass above z215 and the comparatively deeper D215 (Fig. 5 c1). What's intriguing is a presence of strong variation in ZSS off Jaigarh (σ , 3.24 gm m^{-2}) highest among all locations although the seasonal variation in chl-a biomass (Fig. 5 c2) is visibly non-existent (σ , 0.05 mg m^{-3}) and lowest among all locations. This is an exact opposite scenario of Kanyakumari, where an insignificant seasonal variation in ZSS is seen even though the chl-a biomass varies strongly. Starting from Kollam (Fig. 5 f1) and moving northward to Jaigarh (Fig. 5 c1), we see that the core of high zooplankton biomass gradually shifts from summer (off Kollam) to winter monsoon (off Jaigarh), with the transition of upper ocean zooplankton biomass happening along Udupi and Goa. On the contrary, chl-a biomass tends to have low seasonal range as we move northward from SEAS, with Jaigarh having the least seasonal variation. This shift along with winter monsoon facilitated deeper thermocline leads to an

241 even larger impact on ZSS.

242 Further north off Mumbai the D215 is deeper in December to early April, resulting in a
243 higher ZSS ([Fig. 5 b2](#)). D23 follows D215 and the oxycline follows an erratic pattern, reaching
244 depths > 140 m during January to March; when a higher biomass is observed above z215. The
245 chl-a biomass shows seasonal variation albeit lower than the SEAS counterpart. At the northern-
246 most site of EAS i.e, off Okha, biomass above z175 is much weaker leading to a relatively lower
247 ZSS ([Fig. 5 a1, a2](#)) compared to Mumbai. There's two chl-a peak off Okha, one in February due to
248 convective mixing induced deepening of MLD [[Wiggert et al., 2005](#), [Lévy et al., 2007](#), [Keerthi et al.,](#)
249 [2017](#), [Shankar et al., 2016](#)] and the other during August in summer monsoon [[Wiggert et al., 2005](#),
250 [Lévy et al., 2007](#)]. The ZSS remains flat during June to September, although the chl-a biomass
251 increases in this time. Afterwards, ZSS gradually increases and attains its maximum in February
252 same as the chl-a biomass. For a discussion on comparison with A22 climatology, the readers are
253 referred section S1 of supplementary.

254 3.3 Seasonal cycle and variability

255 This section will deal with a discussion on the seasonal cycle and variability of biomass and ZSS
256 in annual and intra-annual scale along the three regimes of EAS. To understand the variation at
257 a specific period, say 365-days (annual cycle) or 180-days (semi-annual cycle), wavelet analysis is
258 carried out for biomass ([Fig. 6](#)) and ZSS ([Fig. 7](#)). However, if we wish to understand the variation
259 in a specific period band, we use Lanczos filtered time series. A brief discussion on the above
260 mentioned techniques and variability in distinct period band is given in section S2.

261 From the linear equation correlating biomass and backscatter, the upper and lower bound of
262 error limits equals to ~ 14 mg m $^{-3}$ ([Fig. 2](#)). The standard deviation of intra-annual (annual)

263 variability is comparable to (less than) the error range of biomass vs backscatter relation. However,
264 we are limited by the gaps in time series as discussed in [section 2.2.1](#). Therefore, we consider
265 locations other than Okha and Jaigarh for the 40 m biomass and ZSS in annual scale.

266 The seasonal cycle is the sum total of annual, semi-annual cycle and their variability. The
267 annual cycle of biomass off Kanyakumari (Udupi and Kollam) is weak (strong), but it varies in
268 time ([Fig. 6](#)). For example off Kollam, the wavelet power is stronger post 2020. Wavelet analysis of
269 the ZSS time series, derived from integrated biomass between 24 and 120 meters depth, indicates
270 absence (presence) of annual cycle off Kanyakumari (off Udupi) ([Fig. 7 g1](#)). To capture the annual
271 variability, the biomass is passed through Lanczos filter within period of 300 to 400 days ([Fig. 8](#)). The
272 annual variability off Kanyakumari is least among all mooring sites. Kollam shows strong annual
273 variability indicating prominent year-to-year variation of biomass. The intra-annual band ([Fig. 9](#))
274 tends to be stronger compared to the annual band. Much like the annual cycle, the semi-annual
275 cycle is weak and intra-annual variability is moderate off Kanyakumari compared to Kollam and
276 Udupi. However, the strong variability in intra-annual scale is restricted to upper ocean for few
277 years off Kollam, where minor spectra around 120 days is also observed.

278 Off Goa, the annual cycle of biomass is comparatively weak contrary to the results of A22,
279 possibly due to shorter time record and low biomass in the recent years as reflected in its ZSS
280 wavelet for 2018 to early 2020 (2021 and 2022) ([Fig. 7](#)) resulting in a weak (strong) annual variability
281 ([Fig. 8](#)). Off Goa and Jaigarh, the semi-annual cycle tends to be strong, specifically during 2022
282 when a anomalous bloom is observed throughout EAS. The semi-annual cycle weakens with depth
283 in these locations. Intra-annual component of seasonal cycle is observed off Goa, with weak (strong)
284 variability during 2019 (2020, 2022) and is moderately strong off Jaigarh ([Fig. 9](#)). Energy is spread
285 among all intra-annual periods for 2022 off Goa ([Figs. 6 and 7](#)), while during 2019 and 2020 the

286 wavelet energy is only present in the semi-annual periods resulting in a overall weaker intra-annual
287 component ([Fig. 6](#)).

288 Further north, a strong annual cycle is seen off Mumbai with strong annual variability highest
289 among EAS sites ([Fig. 8](#)). Biomass variability in annual scale decreases minutely with depth off
290 Mumbai and the three CEAS sites than off Kollam ([Fig. 8](#)) similar to the observed ocean currents
291 [[Chaudhuri et al., 2020, 2021](#)]. The annual cycle and annual variability of biomass and subsequently,
292 ZSS increases along the slope as we go northward to Mumbai from Kanyakumari. The intra-annual
293 band's strength is reduced off Mumbai and Okha as compared to CEAS and SEAS, and the intra-
294 annual variability also decreases more with depth as we go equatorward. The semi-annual cycle is
295 moderately present at 40 m off Mumbai which weakens at 104 m resulting in higher contribution of
296 annual cycle to ZSS. Analysis reveals the presence of moderately strong semi-annual cycle off Okha
297 but only at 104 m and it's intra-annual (annual) band is similar (weaker) in magnitude as compared
298 to Mumbai. Excluding Kanyakumari, intra-annual variability of biomass decreases poleward with
299 higher variation seen off Kollam and Udupi similar to the WICC [[Amol et al., 2014, Chaudhuri](#)
300 [et al., 2020](#)].

301 4 Interannual variability

302 Aberrations from the seasonal cycle occurs due to the variations in interannual and intraseasonal
303 scales, we deal with the former (later) in this (next) section. The presence of interannual variability
304 in zooplankton biomass is not well observed or understood previously due to lack of continuous
305 long-term data. Unlike previous studies [[Madhupratap et al., 1996a, Jyothibabu et al., 2010](#)], the
306 work carried out using long continuous time series by A22 was able to shed light on the seasonal
307 cycle and hinted on the strong interannual variability at Kollam, a feature that was not seen at rest

308 of the sites. We've used the latest ADCP records along with data used in A22 off Mumbai, Goa,
309 and Kollam to show strong presence of interannual variability.

310 From the biomass time series off Kollam, a higher biomass is observed for the years 2016, 2018–
311 2019, and 2022–2023 ([Fig. 3](#)) with deeper D215. It is low for the years 2013 and to a great extent
312 during 2020 and the D215 is shallow enough to touch depths up to ~20 m and above throughout
313 the year. This reason led us to discard D215 for 2020 in our analysis. The higher and lower
314 biomass extending years is coming from the underlying interannual variability of biomass ([Fig. S2](#)).
315 The magnitude of interannual component is higher than the annual variability, and it masks the
316 underlying weaker annual component irrespective of whether it is strongly positive or negative as
317 seen in the monthly resampled biomass time series ([Fig. S2](#)). The wavelet spectra of daily biomass
318 at 40 m is able to register the quasi-biennial oscillations (~720 days) observed in this time series.
319 Off Goa however, the biomass doesn't show much year-to-year variations resulting in lack of spectra
320 within the Cone of Influence (CoI), but the spectra shows up at seasonal and intraseasonal scales.
321 Further north, Mumbai have the strongest observed annual cycle as discussed using recent data
322 ([Fig. 6](#)), but the appended data from A22 shows evidence of variability at ~720 days ([Fig. S2](#)).
323 The variability off Kanyakumari as inferred from it's biomass time series is similar to that of
324 off Kollam, such as during 2020 when both the sites had low biomass year round, but since the
325 mean biomass at any given depth above its z175 is lower than the z215 off Kollam, the impact of
326 interannual variability is reflected prominently at the later site.

327 5 Intraseasonal variability

328 On the similar lines as discussed in the preceding section, intraseasonal variability of biomass is
329 defined as shifts occurring within a season, typically lasting few days to few weeks and is driven

330 by short-term environmental changes, e.g., nutrient replenishment (depletion) in short-span due to
331 upwelling and/or entrainment (bloom). The variability can be split into two categories; a high-
332 frequency (period < 30 days) and a low-frequency (30 < period < 90 days) component. The
333 presence of significant variation in the 30-day running mean with recurring bursts are seen in the
334 daily data and in the wavelet analysis of biomass at 40 and 104 m ([Fig. 6](#)) lasting few days to
335 a week and distinctive to each location. Most of the spikes in biomass are occurring due to the
336 high-frequency component of intraseasonal band, but our focus is on the low-frequency component
337 seen as bursts lasting much longer than biomass spikes. Much like the intra-annual variability,
338 the standard deviation of intraseasonal component is comparable or higher than the error range of
339 unfiltered biomass vs backscatter relation.

340 5.1 Intraseasonal variability of biomass

341 The strength and contribution of variability components changes over time and differs between EAS
342 regimes as discussed in [section 3.3](#). From the wavelet analysis of biomass at 40 and 104 m, peaks
343 in low-frequency intraseasonal band is observed across EAS. But the variability can be different at
344 upper and lower regimes at a given location within a specific period band. This difference is evident
345 e.g., during 2019–2021 off Kanyakumari, the wavelet power of biomass within the intraseasonal
346 band declines as we go deeper from 40 m ([Fig. 6](#)). The filtered biomass in intraseasonal band also
347 showcases the decrease in variability with respect to depth for the same period off Kanyakumari
348 ([Fig. 10](#)). This holds true across EAS with the exception of very few years where the variability
349 at 104 m is comparable or higher than biomass variability at surface layers. However, in other few
350 instances, such as during September–November of 2018 off CEAS, intraseasonal variability remains
351 consistent throughout the entire water column.

352 Strong intraseasonal variability off Kanyakumari relative to the variability in its annual band,
353 along-with comparable or lower range of intra-annual variability ([Fig. 11](#)) and the wavelet at 40
354 and 104 m indicates that the short-lived environmental changes is a major driver of its biomass
355 alongside minor seasonal variation. Off Kollam and Udupi, the presence of intraseasonal bursts is
356 prominent, but due to an equal strength of intra-annual component the biomass isn't solely driven
357 by short-term environmental changes. For instance, in 2019 off Kollam ([Fig. 11](#)), low frequency
358 intraseasonal variability was weak during summer monsoon but an increase in biomass during the
359 same period was due to an increase intra-annual component. However, a sharp decline in August
360 2019 resulted from reduced intra-annual and intraseasonal variability, even with the presence of a
361 weakly positive annual variability.

362 Off Goa, strong peaks in intraseasonal band is present in wavelet spectra of biomass. During
363 early 2019 to late 2020, the intra-annual variability off Goa is non-existent and with the weak
364 annual variability ([Fig. 11](#)), a rather seasonally invariant biomass at 40 and 104 m is observed but
365 the presence of intraseasonal variations is seen at both 40 and 104 m ([Fig. 4](#)). The wavelet peaks in
366 intraseasonal band occurred strongly in 2018 and later in 2020, but the absence intra-annual band in
367 2019 makes it easier to comprehend the contribution of intraseasonal variability. A similar feature
368 is noted off Jaigarh albeit with a weaker magnitude. Weak presence of intraseasonal variability is
369 noticed in the relatively smoother 30-day rolling mean biomass off Mumbai and Okha. During early
370 2021 off Mumbai, the presence of strong intraseasonal peaks in wavelet spectra of 104 m along with
371 40 m ([Fig. 6](#)) shows up in biomass variability in intraseasonal scale ([Fig. 10](#)). Although spectra
372 in the intraseasonal band is present at 40 m off Mumbai and Okha, it is almost absent at 104 m
373 except for a select few years. It implies that at some locations the strong variability may occur at
374 deeper depth even when the upper ocean is showing lower variability. Off Okha, the intraseasonal

³⁷⁵ variability is lowest among all EAS sites followed by Mumbai. However, Okha has weak annual and
³⁷⁶ intra-annual variability unlike Mumbai leading to least predictability.

³⁷⁷ 5.2 Intraseasonal variability of standing stock

³⁷⁸ The biomass variability at 40 and 104 m in intraseasonal scale is well reflected in the ZSS time series
³⁷⁹ and the corresponding wavelet spectra ([Fig. 7](#)). While 40 m biomass varies strongly Off SEAS, the
³⁸⁰ biomass variation at 104 m is weaker in comparison leading to upper ocean determined ZSS. There
³⁸¹ are instances when both 40 and 104 m biomass are in phase leading to a stronger ZSS variation
³⁸² e.g., September–November 2019 off Kanyakumari ([Fig. S3](#)) though biomass variation at 104 m is
³⁸³ weak ([Fig. 10](#)). At instances such as during June–July 2018 and Mar–July 2019 at the above
³⁸⁴ location, when the 40 and 104 m biomass are anti-phase or not in phase, they result in a reduced
³⁸⁵ ZSS ([Fig. S3](#)). No annual and semi-annual cycle seems to be present in ZSS off Kanyakumari, but
³⁸⁶ presence of bursts lasting few days to weeks are an indication of intraseasonal variations. While
³⁸⁷ off Kollam and Udupi, the presence of strong intra-annual variations is observed in ZSS alongside
³⁸⁸ intraseasonal variation dominant during September–November. Off Goa and Jaigarh during early
³⁸⁹ 2019 to late 2020, the intra-annual and annual variations are much weak but strong intraseasonal
³⁹⁰ variation leads to bursts in biomass. The resulting ZSS at these locations shows strong intraseasonal
³⁹¹ bursts but seasonal variation is weaker (([Fig. 7](#)) d2, c2). Strength of intraseasonal variability in
³⁹² biomass is reduced at NEAS ([Fig. 10](#)) leading to a comparatively smoother ZSS in 30-day rolling
³⁹³ mean data ([Fig. 7](#) a2, b2).

³⁹⁴ The intraseasonal peaks in biomass and further ZSS are strong in SEAS followed by CEAS and
³⁹⁵ is weak off NEAS sites ([Fig. 10](#)). Variability in intraseasonal scale seems to occur predominantly
³⁹⁶ during August to November, for example off Kanyakumari (2018, 2019 and 2020), off Kollam (2018,

2021 and 2022) and off Udupi (2018) although it can extend to mid-summer/mid-winter monsoon
for few years and is coherent along much of the EAS slope as seen during 2018 at intraseasonal band
or sometimes even at scale of few days (Fig. 11). The coherence and strong variability at deeper
depths at instance (during early 2021 off Mumbai) indicates possible role of ocean circulation in
determining biomass at intraseasonal periods. Also, the magnitude of intraseasonal variability of 40
m (104 m) biomass decreases (increases) as we move poleward (Fig. 11), the 40 m variance is much
like the observed intraseasonal currents [Amol et al., 2014, Chaudhuri et al., 2020, 2021]. However,
the strength of intraseasonal variability of biomass is in contrast to the corresponding band of
WICC which is strong during winter monsoon along the slope [Amol et al., 2014, Chaudhuri et al.,
2020] and shelf [Chaudhuri et al., 2021] suggesting further study to identify any possible connection.
Nonetheless, the backscatter derived biomass in higher sampling frequency is essential for discussing
the intraseasonal variability, whereas conventional sampling method such as with research vessel,
where one snapshot of biomass is taken in an interval of 15–30 days, would fail to capture these
bursts in biomass.

6 Discussion

6.1 Summary

The zooplankton biomass and standing stock across different regions of EAS was examined in this article, highlighting their spatio-temporal trends in the light of physico-chemical parameters using the multi-yearlong ADCP backscatter data from 2017 to 2023.

The findings shows notable seasonal variation in zooplankton biomass and ZSS; in SEAS the higher biomass is observed during summer monsoon, while in NEAS the high biomass is observed

418 during winter monsoon with transition of peak biomass happening gradually along CEAS ([section 3.2](#)). Off Kollam, a unique double peak in ZSS occurs, one during May to July and another in
419 September to November, suggesting a complex interplay between environmental drivers and zooplankton growth ([Fig. 5 f2](#)). Off Kanyakumari, the seasonal variation in ZSS is non-existent even
420 though a dramatic seasonality is seen in chl-a. On contrary, Jaigarh shows strong variation in ZSS
421 where the chl-a variation is non-existent. Such feature was observed at embayment west off Antarctic
422 peninsula and has been attributed to advective influx [[Espinasse et al., 2012](#)] but the distinct
423 dynamics of EAS and Antarctica implies the causality may not be same. Climatology shows strong
424 decline in biomass w.r.t. depth off Goa, then NEAS sites off Jaigarh, Mumbai and Okha followed
425 by SEAS locations off Udupi, Kollam and Kanyakumari. The minor peak observed off Mumbai in
426 A22's climatology is absent in the climatology presented using the recent data.

427 Seasonal cycle and variability play a crucial role in regulating biomass. A strong annual cycle
428 is observed at NEAS ([Fig. 6](#)), with biomass peaking during winter monsoon months ([Fig. 5](#)) and
429 deeper D215, the annual cycle weakens as we got equatorward. CEAS and SEAS regions particularly
430 off Kollam, exhibit more complex patterns. Off Kollam, the presence of a weak annual cycle and
431 a stronger semi-annual cycle is noted along with a strong quasi-biennial cycle agreeing with A22.
432 The semi-annual cycle is especially prominent in the SEAS ([section 3.3](#)), where it contributes
433 significantly to the seasonal biomass changes. The variability in annual scale is weak, while that
434 in intra-annual scale is often comparable to intraseasonal variability which is found to influence
435 zooplankton biomass strongly in the summer to winter monsoon transition months ([Fig. 10](#)). The
436 high (low) frequency component of intraseasonal variability determine changes lasting for days (few
437 days to weeks) observed as spikes (bursts) in the daily biomass record ([Fig. 11](#)). Intraseasonal
438 variability is higher in the SEAS, with the NEAS displaying less variance. The intraseasonal
439 variability is higher in the SEAS, with the NEAS displaying less variance. The intraseasonal
440 variability is higher in the SEAS, with the NEAS displaying less variance.

variability is often restricted to the upper layer, and it is expected owing to higher variability of chl-a at surface which weakens with increasing depth. The affect of intraseasonal variability compounded with presence of strong intra-annual is observed in the difference of mean biomass at 40 and 104 m ([Fig. 4](#)). The intraseasonal variations may exist throughout the water column for few years and can be coherent along the slope possibly suggesting that the penetration and propagation of currents in intraseasonal band [[Amol et al., 2012, 2014, Chaudhuri et al., 2020](#)]) could be driving biomass on few occasions. The reduction/enhancement of ZSS on account of out-of-phase/in-phase upper and lower depth biomass occurs at annual and intra-annual and intraseasonal time scales ([Fig. S3](#)).

6.2 consequences of intraseasonal variability

It is evident that the intraseasonal variability dominates the zooplankton biomass along EAS regime ([section 5](#)). A strong intraseasonal component suggests implications on sampling, zooplankton patchiness and its predictability.

6.2.1 Implication on sampling

Zooplankton biomass exhibits significant intraseasonal variability driven by dynamic oceanographic processes which operate over short temporal scales and vary in space ([section 5](#)). Since the strength of intraseasonal component is higher than the other two variabilities ([Fig. 11](#)) and its high-frequency component is rather erratic, dependency of zooplankton biomass on the intra-seasonal variation has implication on the sampling of zooplankton using cruises. A servicing cruise along the EAS moorings takes about 12 to 15 days excluding the time to and fro from port to first/last mooring [[Chaudhuri et al., 2020, Aparna et al., 2022](#)]. However, a sampling cruise dedicated to study the

⁴⁶² spatial variation of zooplankton [Madhupratap et al., 1992, Smith et al., 1998, Wishner et al., 1998,
⁴⁶³ Kidwai and Amjad, 2000], say for summer monsoon may last a month or more with coarse sampling
⁴⁶⁴ interval and hence fail to capture the actual biomass within a season for a fair spatial comparison.

⁴⁶⁵ Consider the cruise undertaken to address the seasonality in zooplankton abundances and com-
⁴⁶⁶ position [Madhupratap et al., 1996a] in Arabian Sea as part of JGOFS program. The first, second
⁴⁶⁷ and third cruises of this study was taken 12 April to 12 May 1994 (inter-monsoon), 3 February to
⁴⁶⁸ 4 March 1995 (winter) and 20 July to 12 August 1995 (summer), respectively. It is imperative to
⁴⁶⁹ acknowledge that sampling done twice (once in mid-day and again in mid-night), and two snapshots
⁴⁷⁰ are held as a representative of the entire season. Does this sampling method give accurate idea
⁴⁷¹ about the zooplankton biomass in a particular season? The comparison of variability in intrasea-
⁴⁷² sonal periods is used to shed a light on the biomass variation within a season. Consider the summer
⁴⁷³ monsoon months, off Mumbai during early June of 2019 (Fig. 11), where a spike in biomass is
⁴⁷⁴ observed due to an instantaneous increase in the high-frequency component of biomass variability
⁴⁷⁵ resulting in an increase of $\sim 150 \text{ mg m}^{-3}$ within few days. Similar spikes are seen at other locations
⁴⁷⁶ too, e.g., off Kollam during July end and multiple instances in September of 2019 (Fig. 11). These
⁴⁷⁷ spikes lasts only for a day to few days but the bursts in biomass tend to last longer from a few
⁴⁷⁸ days to a few weeks. A burst is seen in biomass during September 2019 off Kanyakumari, but
⁴⁷⁹ the preceding summer monsoon months had an almost invariant biomass with minor bursts, both
⁴⁸⁰ of which won't be captured by a conventional ship based sampling. Second limitation of cruise
⁴⁸¹ based sampling is spatial constraint. For the same year 2019 off Kanyakumari, the burst in biomass
⁴⁸² during September is followed by a decline during October which results in a biomass difference of
⁴⁸³ about $\sim 160 \text{ mg m}^{-3}$ within a month and most of it is contribution from intraseasonal variability
⁴⁸⁴ (Fig. 11). This burst is also observed off Kollam, Udupi till Goa, albeit with decreasing intensity

as we go poleward. Such coherency can only be observed if continuous and frequent measurements were taken across EAS. The spatial map of mesozooplankton distribution such as one by Jyothibabu et al. [2010] for each season (see Fig. 11 of Jyothibabu et al. [2010]) is limited by sampling frequency and time elapsed to cover stations, and the measured biomass is prone to distortion since biomass is subject to drastic changes within few days. The limitations of cruise based sampling leads to inaccurate depiction of biomass in space and time, and it can be mitigated by usage of ADCP backscatter derived zooplankton biomass.

6.2.2 Zooplankton patchiness

Poor sampling coverage and intermittent measurement also impacts assessment of zooplankton patchiness, defined as the aggregations arising in response to temperature, salinity and oxygen gradients, currents, variation in light intensity, predator-prey concentrations [Folt and Burns, 1999, Raghukumar and Anil, 2003]. Though the usage of traditional sampling methods has led to determination of zooplankton abundance and distribution in EAS [Madhupratap et al., 1992, 1996a, Khandagale et al., 2022], the biomass measurements can miss or rarely sample the patches of zooplankton, and thereby misinterpret abundance by under/over-estimation of the standing stock. A high intraseasonal variability in zooplankton biomass suggests that patchiness in the deep-sea environment occurs within individual seasons on periods equivalent to few days to few weeks. During July 20–31st 2019, a spike lasting few days in daily biomass at 40 m (Fig. 11) is observed at most of the EAS sites, albeit with differing magnitude followed by a sharp decline and difference in occurrence of maximum biomass by few days. But the coherence doesn't exist at all instances. For example, during 13th June 2019, the instantaneous spike in biomass observed off Mumbai is not seen anywhere else, but the low biomass lasting about 2 weeks in dates adjacent to this spike is

seen at Okha, Mumbai, Jaigarh and Goa (Fig. 11). The observed spikes in zooplankton biomass, as discussed in the preceding subsection, occurring within just a few days, are a clear example of the zooplankton cluster formation. The patchiness can also exist on longer periods. During 15 January–15 February 2019, a burst is observed off Udupi lasting about 20–30 days, while it is missing at its nearby moorings, signifying presence of patchiness and its prominence in the longer periods of intraseasonal band. However, there are occasions such as during September–November 2018 (Fig. 10) and 2019 (Fig. 11) when the coherence in biomass is observed indicating collapse of patchiness.

The zooplankton patchiness occurring in longer periods of intraseasonal band is likely associated with processes such as fronts [Coyle and Jr, 2000, Wade and Heywood, 2001, Hitchcock et al., 2002], pulsed inputs of nutrients in open ocean water [Anil et al., 2021] and biological processes [Folt and Burns, 1999], while those occurring in shorter periods could be due to physical convergence [Napp et al., 1996] of zooplankton. The higher variance in deeper layers off Okha could be an indication of deep-living zooplankton species [Raghukumar and Anil, 2003] due to strong oxygen gradient. Thus, a lack of feasibility in intensive in-situ sampling suggests that the data collected might not be representative of the actual standing stock being studied [Smith et al., 1998] and may not capture zooplankton patches.

6.2.3 Predictability

Though EAS shows a strong seasonal cycle of current, there are notable differences between regimes of EAS. Kollam's seasonal cycle is marked by intense intraseasonal bursts making the shelf WICC at Kollam highly unpredictable [Chaudhuri et al., 2021] and the intraseasonal variability increases equatorward. The direction of WICC at any given time of the year can be either poleward or

equatorward owing to the bursts. Similarly, the zooplankton biomass varies frequently and strongly within the season itself ([section 5](#)) across EAS. From the preceding subsection, it is inferred that though not often, coherence is observed in both the lower and higher periods of intraseasonal band leading to collapse of patchiness. The presence of coherence implicates better predictability of biomass especially during September–November as observed during 2018 and 2019. However, rest of the time in absence of coherence in few months, patchiness takes over and the zooplankton biomass is erratic with sudden spikes and lasting bursts. This indicates that zooplankton form and patches fluctuate due to short-term changes, possibly responding to ocean environment [[Folt and Burns, 1999](#), [Raghukumar and Anil, 2003](#), [Anil et al., 2021](#)]. Hence, the zooplankton biomass much like the current is dominated by intraseasonal variations more than the annual cycle indicating possible loss in predictability.

Understanding the currents and phytoplankton variability and their relation to zooplankton would enable us to have better predictability. The occurrence of strong biomass intraseasonal variability before winter monsoon, the similarity in trend of increasing (decreasing) intraseasonal and intra-annual (annual) variability of biomass and currents as we go equatorward along the EAS slope, presence strong interannual variability in biomass and currents and quasi-biennial cycle that is associated with Indian summer-monsoon rainfall [[Mooley and Parthasarathy, 1984](#), [Bhalme et al., 1987](#), [Meehl and Arblaster, 2002](#)], all these are tempting as it indicates a link between the two. However, a rigorous study is necessary to excavate any such relationship. Strong peaks in intraseasonal band in chl-a was evident in Lomb–Scargle periodogram (figure not shown), analogous to zooplankton biomass and ZSS, but lacked concrete evidence of direct correlation.

550 **6.3 Conclusion**

551 The results presented in this paper are based on the ADCP backscatter which is suitable for creating
552 long-term time series of zooplankton biomass in open ocean [Jiang et al., 2007, Hobbs et al., 2021,
553 Ursella et al., 2021, Aparna et al., 2022]. There are however, certain limitations to this approach
554 of studying biomass using ADCP backscatter as proxy. While the variation in depth is captured
555 with in-situ samples from MPN, the variation in season is not adequately addressed owing to the
556 limitation of months when ADCP servicing cruises are undertaken apart from availability. The west
557 coast cruises for ADCP servicing are planned for the monsoon transition months but may start as
558 early as late September till December with few exceptions such as 2022 when it was carried out
559 in March. Since the intraseasonal and intra-annual variability is almost double that of the annual
560 one (section 5), the sampling done in particular season for biomass-backscatter comparison isn't
561 sufficient but can be mitigated with extensive season-wise sampling [Jadhav and Smitha, 2024].
562 The second limitation is lack of any information regarding the size distribution of zooplankton and
563 their contribution to ZSS is lost.

564 The merits outshine above mentioned disadvantages in the unique aspect that a sufficiently
565 long and continuous time series of zooplankton biomass could be constructed upon which further
566 analysis can be carried out. Along-with the discussion on seasonal and further the climatological
567 cycle, we provided evidence of strong intraseasonal variation; this has three major implications:
568 1) on the conventional sampling methods used to assess the zooplankton biomass and standing
569 stock, and the snapshots provided by such samples aren't representative of a season; 2) on the
570 zooplankton patchiness, and further on the under or over estimation of standing stock; 3) on the
571 predictability which is reduced due to strong biomass variation at intraseasonal scale, and the
572 presence of patchiness as spikes and bursts. The possible influence of ocean currents could be

573 explored using the current data from ADCPs [Hitchcock et al., 2002, Lawson et al., 2004]. It is
574 evident that a mono-frequency ADCP is adequately suitable to capture the intraseasonal variations
575 of zooplankton biomass that will otherwise be left inaccessible by traditional methods.

576 7 Declaration of competing interest

577 The authors declare that they have no known competing financial interests or personal relationships
578 that could have appeared to influence the work reported in this paper.

579 8 Acknowledgments

580 The data were collected by xxx with fund provided under xxxx. The mooring programme is
581 supported by INCOIS (Indian National Centre for Ocean Information Services, Hyderabad) and
582 CSIR. We acknowledge the contribution of mooring division and ship cell of CSIR-NIO.

583 Ranjan Kumar Sahu expresses his acknowledgment to the Council of Scientific and Industrial
584 Research (CSIR) for sponsoring his fellowship. Additionally, he extends his thanks to Ashok
585 Kankonkar for providing the essential data, Rahul Khedekar for his data processing, Roshan D'Souza
586 for his diligent work in biological data analysis. Their contributions were invaluable to the successful
587 completion of this research.

588 References

- 589 Anna-Karin Almén and Tobias Tamlander. Temperature-related timing of the spring bloom and match between
590 phytoplankton and zooplankton. *Marine Biology Research*, 16(8-9):674–682, 2020.
- 591 P Amol, D Shankar, SG Aparna, SSC Shenoi, V Fernando, SR Shetye, A Mukherjee, Y Agarvadekar, S Khalap, and
592 NP Satelkar. Observational evidence from direct current measurements for propagation of remotely forced waves
593 on the shelf off the west coast of india. *Journal of Geophysical Research: Oceans*, 117(C5), 2012.

- 594 P Amol, D Shankar, V Fernando, A Mukherjee, SG Aparna, R Fernandes, GS Michael, ST Khalap, NP Satelkar,
595 Y Agarvadekar, et al. Observed intraseasonal and seasonal variability of the west india coastal current on the
596 continental slope. *Journal of Earth System Science*, 123(5):1045–1074, 2014.
- 597 P Amol, Suchandan Bemal, D Shankar, V Jain, V Thushara, V Vijith, and PN Vinayachandran. Modulation of
598 chlorophyll concentration by downwelling rossby waves during the winter monsoon in the southeastern arabian
599 sea. *Progress in Oceanography*, 186:102365, 2020.
- 600 AC Anil, DV Desai, L Khandeparker, V Krishnamurthy, K Mapari, S Mitbavkar, JS Patil, VVSS Salma, and
601 SS Sawant. Short term response of plankton community to nutrient enrichment in central eastern arabian sea:
602 Elucidation through mesocosm experiments. *Journal of Environmental Management*, 288:112390, 2021.
- 603 SG Aparna, DV Desai, D Shankar, AC Anil, Shrikant Dora, and R Khedekar. Seasonal cycle of zooplankton standing
604 stock inferred from adcp backscatter measurements in the eastern arabian sea. *Progress in Oceanography*, 203:
605 102766, 2022.
- 606 K Banse and DC English. Geographical differences in seasonality of czcs-derived phytoplankton pigment in the
607 arabian sea for 1978–1986. *Deep Sea Research Part II: Topical Studies in Oceanography*, 47(7-8):1623–1677, 2000.
- 608 Karl Banse. Hydrography of the arabian sea shelf of india and pakistan and effects on demersal fishes. In *Deep sea*
609 *research and oceanographic Abstracts*, volume 15, pages 45–79. Elsevier, 1968.
- 610 Karl Banse. Zooplankton: pivotal role in the control of ocean production: I. biomass and production. *ICES Journal*
611 *of marine Science*, 52(3-4):265–277, 1995.
- 612 Richard T Barber, John Marra, Robert C Bidigare, Louis A Codispoti, David Halpern, Zackary Johnson, Mikel
613 Latasa, Ralf Goericke, and Sharon L Smith. Primary productivity and its regulation in the arabian sea during
614 1995. *Deep Sea Res. Part 2 Top. Stud. Oceanogr.*, 48(6-7):1127–1172, jan 2001.
- 615 H. P. Batchelder, J. R. VanKeuren, R. D. Vaillancourt, and E. Swift. Spatial and temporal distributions of acoustically
616 estimated zooplankton biomass near the marine light-mixed layers station ($59^{\circ}30'N$, $21^{\circ}00'W$) in the north atlantic
617 in may 1991. *Journal of Geophysical Research: Oceans*, 100:6549–6563, 1995. doi: 10.1029/94jc00981.
- 618 Suchandan Bemal, Arga Chandrashekhar Anil, D Shankar, R Remya, and Rajdeep Roy. Picophytoplankton variability:
619 Influence of winter convective mixing and advection in the northeastern arabian sea. *Journal of Marine Systems*,
620 180:37–48, 2018.
- 621 HN Bhalme, SS Rahalkar, and AB Sikder. Tropical quasi-biennial oscillation of the 10-mb wind and indian monsoon
622 rainfall-implications for forecasting. *Journal of climatology*, 7(4):345–353, 1987.
- 623 John C Brock and Charles R McClain. Interannual variability in phytoplankton blooms observed in the northwestern
624 arabian sea during the southwest monsoon. *Journal of Geophysical Research: Oceans*, 97(C1):733–750, 1992.

- 625 John C Brock, Charles R McClain, Mark E Luther, and William W Hay. The phytoplankton bloom in the north-
626 western arabian sea during the southwest monsoon of 1979. *Journal of Geophysical Research: Oceans*, 96(C11):
627 20623–20642, 1991.
- 628 Abhisek Chatterjee, D Shankar, SSC Shenoi, GV Reddy, GS Michael, M Ravichandran, VV Gopalkrishna,
629 EP Rama Rao, TVS Udaya Bhaskar, and VN Sanjeevan. A new atlas of temperature and salinity for the north
630 indian ocean. *Journal of Earth System Science*, 121:559–593, 2012.
- 631 Anya Chaudhuri, D Shankar, SG Aparna, P Amol, V Fernando, A Kankonkar, GS Michael, NP Satelkar, ST Khalap,
632 AP Tari, et al. Observed variability of the west india coastal current on the continental slope from 2009–2018.
633 *Journal of Earth System Science*, 129(1):57, 2020.
- 634 Anya Chaudhuri, P Amol, D Shankar, S Mukhopadhyay, SG Aparna, V Fernando, and A Kankonkar. Observed
635 variability of the west india coastal current on the continental shelf from 2010–2017. *Journal of Earth System
636 Science*, 130:1–21, 2021.
- 637 Boris Cisewski, Volker H Strass, Monika Rhein, and Sören Krägesky. Seasonal variation of diel vertical migration
638 of zooplankton from adcp backscatter time series data in the lazarev sea, antarctica. *Deep Sea Research Part I:
639 Oceanographic Research Papers*, 57(1):78–94, 2010.
- 640 Kenneth O Coyle and George L Hunt Jr. Seasonal differences in the distribution, density and scale of zooplankton
641 patches in the upper mixed layer near the. *Plankton Biol. Ecol*, 47(1):31–42, 2000.
- 642 Kent L Deines. Backscatter estimation using broadband acoustic doppler current profilers. In *Proceedings of the
643 IEEE Sixth Working Conference on Current Measurement (Cat. No. 99CH36331)*, pages 249–253. IEEE, 1999.
- 644 SN DeSousa, M Dileepkumar, S Sardessai, VVSS Sarma, and PV Shirodkar. Seasonal variability in oxygen and
645 nutrients in the central and eastern arabian sea. Indian Academy of Sciences, 1996.
- 646 A Edvardsen, D Slagstad, KS Tande, and P Jaccard. Assessing zooplankton advection in the barents sea using
647 underway measurements and modelling. *Fisheries Oceanography*, 12(2):61–74, 2003.
- 648 Boris Espinasse, Meng Zhou, Yiwu Zhu, Elliott L Hazen, Ari S Friedlaender, Douglas P Nowacek, Dezhong Chu,
649 and Francois Carlotti. Austral fall- winter transition of mesozooplankton assemblages and krill aggregations in an
650 embayment west of the antarctic peninsula. *Marine Ecology Progress Series*, 452:63–80, 2012.
- 651 Charles N Flagg and Sharon L Smith. On the use of the acoustic doppler current profiler to measure zooplankton
652 abundance. *Deep Sea Research Part A. Oceanographic Research Papers*, 36(3):455–474, 1989.
- 653 Carol L Folt and Carolyn W Burns. Biological drivers of zooplankton patchiness. *Trends in Ecology & Evolution*,
654 14(8):300–305, 1999.
- 655 H. E. García, R. A. Locarnini, T. P. Boyer, J. I. Antonov, A. V. Mishonov, O. K. Baranova, M. M. Zweng, J. R.
656 Reagan, and D. R. Johnson. Dissolved oxygen, apparent oxygen utilization, and oxygen saturation. *NOAA Atlas
657 NESDIS 75*, 3, 2014.

- 658 Charles H Greene, Peter H Wiebe, Chris Pelkie, Mark C Benfield, and Jacqueline M Popp. Three-dimensional
659 acoustic visualization of zooplankton patchiness. *Deep Sea Research Part II: Topical Studies in Oceanography*, 45
660 (7):1201–1217, 1998.
- 661 Charles F Greenlaw. Acoustical estimation of zooplankton populations 1. *Limnology and Oceanography*, 24(2):
662 226–242, 1979.
- 663 Davide Guerra, Katrin Schroeder, Mireno Borghini, Elisa Camatti, Marco Pansera, Anna Schroeder, Stefania
664 Sparnocchia, and Jacopo Chiggiato. Zooplankton diel vertical migration in the corsica channel (north-western
665 mediterranean sea) detected by a moored acoustic doppler current profiler. *Ocean Science*, 15(3):631–649, 2019.
- 666 James M Hamilton, Kate Collins, and Simon J Prinsenberg. Links between ocean properties, ice cover, and plankton
667 dynamics on interannual time scales in the canadian arctic archipelago. *Journal of Geophysical Research: Oceans*,
668 118(10):5625–5639, 2013.
- 669 Graeme C Hays. A review of the adaptive significance and ecosystem consequences of zooplankton diel vertical
670 migrations. In *Migrations and Dispersal of Marine Organisms: Proceedings of the 37 th European Marine Biology
671 Symposium held in Reykjavík, Iceland, 5–9 August 2002*, pages 163–170. Springer, 2003.
- 672 Karen J Heywood, S Scrope-Howe, and ED Barton. Estimation of zooplankton abundance from shipborne adcp
673 backscatter. *Deep Sea Research Part A. Oceanographic Research Papers*, 38(6):677–691, 1991.
- 674 Gary L Hitchcock, Peter Lane, Sharon Smith, Jiangang Luo, and Peter B Ortner. Zooplankton spatial distributions
675 in coastal waters of the northern arabian sea, august, 1995. *Deep Sea Research Part II: Topical Studies in
676 Oceanography*, 49(12):2403–2423, 2002.
- 677 Laura Hobbs, Neil S Banas, Jonathan H Cohen, Finlo R Cottier, Jørgen Berge, and Øystein Varpe. A marine
678 zooplankton community vertically structured by light across diel to interannual timescales. *Biology Letters*, 17(2):
679 20200810, 2021.
- 680 Raleigh R Hood, Lynnath E Beckley, and Jerry D Wiggert. Biogeochemical and ecological impacts of boundary
681 currents in the indian ocean. *Progress in Oceanography*, 156:290–325, 2017.
- 682 Ryuichiro Inoue, Minoru Kitamura, and Tetsuichi Fujiki. Diel vertical migration of zooplankton at the s 1 biogeo-
683 chemical mooring revealed from acoustic backscattering strength. *Journal of Geophysical Research: Oceans*, 121
684 (2):1031–1050, 2016.
- 685 Shirin J Jadhav and BR Smitha. Abundance distribution pattern of zooplankton associated with the eastern arabian
686 sea monsoon system as detected by underwater acoustics and net sampling. *Acoustics Australia*, pages 1–22, 2024.
- 687 Songnian Jiang, Tommy D Dickey, Deborah K Steinberg, and Laurence P Madin. Temporal variability of zooplankton
688 biomass from adcp backscatter time series data at the bermuda testbed mooring site. *Deep Sea Research Part I:
689 Oceanographic Research Papers*, 54(4):608–636, 2007.

- 690 R Jyothibabu, NV Madhu, H Habeebrehman, KV Jayalakshmy, KKC Nair, and CT Achuthankutty. Re-evaluation
691 of ‘paradox of mesozooplankton’ in the eastern arabian sea based on ship and satellite observations. *Journal of*
692 *Marine Systems*, 81(3):235–251, 2010.
- 693 Myounghee Kang, Sunyoung Oh, Wooseok Oh, Dong-Jin Kang, SungHyun Nam, and Kyounghoon Lee. Acoustic
694 characterization of fish and macroplankton communities in the seychelles-chagos thermocline ridge of the southwest
695 indian ocean. *Deep Sea Research Part II: Topical Studies in Oceanography*, 213:105356, 2024.
- 696 Madhavan Girijkumari Keerthi, Matthieu Lengaigne, Marina Levy, Jerome Vialard, Vallivattathillam Parvathi,
697 Clément de Boyer Montégut, Christian Ethé, Olivier Aumont, Iyyappan Suresh, Valiya Parambil Akhil, et al.
698 Physical control of interannual variations of the winter chlorophyll bloom in the northern arabian sea. *Biogeosciences*,
699 14(15):3615–3632, 2017.
- 700 Punam A Khandagale, Vaibhav D Mhatre, and Sujitha Thomas. Seasonal and spatial variability of zooplankton
701 diversity in north eastern arabian sea along the maharashtra coast. *Journal of the Marine Biological Association*
702 *of India*, 64(1):25–32, 2022.
- 703 S Kidwai and S Amjad. Zooplankton: pre-southwest and northeast monsoons of 1993 to 1994, from the north arabian
704 sea. *Mar. Biol.*, 136(3):561–571, apr 2000.
- 705 S. Prasanna Kumar and Jayu Narvekar. Seasonal variability of the mixed layer in the central arabian sea and its
706 implication on nutrients and primary productivity. *Deep Sea Research Part II: Topical Studies in Oceanography*,
707 52(14):1848–1861, 2005. ISSN 0967-0645. doi: <https://doi.org/10.1016/j.dsr2.2005.06.002>. URL <https://www.sciencedirect.com/science/article/pii/S0967064505001207>. Biogeochemical Processes in the Northern Indian
708 Ocean.
- 709 Gareth L Lawson, Peter H Wiebe, Carin J Ashjian, Scott M Gallager, Cabell S Davis, and Joseph D Warren.
710 Acoustically-inferred zooplankton distribution in relation to hydrography west of the antarctic peninsula. *Deep
711 Sea Research Part II: Topical Studies in Oceanography*, 51(17-19):2041–2072, 2004.
- 712 Marina Lévy, D Shankar, J-M André, SSC Shenoi, Fabien Durand, and Clément de Boyer Montégut. Basin-wide
713 seasonal evolution of the indian ocean’s phytoplankton blooms. *Journal of Geophysical Research: Oceans*, 112
714 (C12), 2007.
- 715 M Li, A Gargett, and K Denman. What determines seasonal and interannual variability of phytoplankton and
716 zooplankton in strongly estuarine systems? *Estuarine, Coastal and Shelf Science*, 50(4):467–488, 2000.
- 717 Yanliang Liu, Jingsong Guo, Yuhuan Xue, Chalermrat Sangmanee, Huiwu Wang, Chang Zhao, Somkiat Khokiat-
718 tiwong, and Weidong Yu. Seasonal variation in diel vertical migration of zooplankton and micronekton in the
719 andaman sea observed by a moored adcp. *Deep Sea Research Part I: Oceanographic Research Papers*, 179:103663,
720 2022.
- 721 M Madhupratap, P Haridas, Neelam Ramaiah, and CT Achuthankutty. Zooplankton of the southwest coast of india:
722 abundance, composition, temporal and spatial variability in 1987. 1992.

- 724 M Madhupratap, TC Gopalakrishnan, P Haridas, KKC Nair, PN Aravindakshan, G Padmavati, and Shiney Paul.
725 Lack of seasonal and geographic variation in mesozooplankton biomass in the arabian sea and its structure in the
726 mixed layer. *Current science. Bangalore*, 71(11):863–868, 1996a.
- 727 M Madhupratap, S Prasanna Kumar, PMA Bhattathiri, M Dileep Kumar, S Raghukumar, KKC Nair, and N Rama-
728 iah. Mechanism of the biological response to winter cooling in the northeastern arabian sea. *Nature*, 384(6609):
729 549–552, 1996b.
- 730 M Madhupratap, TC Gopalakrishnan, P Haridas, and KKC Nair. Mesozooplankton biomass, composition and
731 distribution in the arabian sea during the fall intermonsoon: implications of oxygen gradients. *Deep Sea Research*
732 *Part II: Topical Studies in Oceanography*, 48(6-7):1345–1368, 2001.
- 733 JP McCreary, Raghu Murtugudde, Jerome Vialard, PN Vinayachandran, Jerry D Wiggert, Raleigh R Hood,
734 D Shankar, and S Shetye. Biophysical processes in the indian ocean. *Indian Ocean biogeochemical processes*
735 and ecological variability
- 736 Julian P McCreary, Pijush K Kundu, and Robert L Molinari. A numerical investigation of dynamics, thermodynamics
737 and mixed-layer processes in the indian ocean. *Progress in Oceanography*, 31(3):181–244, 1993.
- 738 Julian P McCreary, Kevin E Kohler, Raleigh R Hood, and Donald B Olson. A four-component ecosystem model of
739 biological activity in the arabian sea. *Progress in Oceanography*, 37(3-4):193–240, 1996.
- 740 Gerald A Meehl and Julie M Arblaster. The tropospheric biennial oscillation and asian–australian monsoon rainfall.
741 *Journal of Climate*, 15(7):722–744, 2002.
- 742 DA Mooley and B Parthasarathy. Fluctuations in all-india summer monsoon rainfall during 1871–1978. *Climatic*
743 *change*, 6(3):287–301, 1984.
- 744 S Mukhopadhyay, D Shankar, S G Aparna, and A Mukherjee. Observations of the sub-inertial, near-surface east
745 india coastal current. *Cont. Shelf Res.*, 148:159–177, September 2017.
- 746 KKC Nair, M Madhupratap, TC Gopalakrishnan, P Haridas, and Mangesh Gauns. The arabian sea: physical
747 environment, zooplankton and myctophid abundance. 1999.
- 748 PV Nair. Primary productivity in the indian seas. *CMFRI Bulletin*, 22:1–63, 1970.
- 749 Jeffrey M Napp, Lewis S Incze, Peter B Ortner, Deborah LW Siefert, and Lisa Britt. The plankton of shelikof strait,
750 alaska: standing stock, production, mesoscale variability and their relevance to larval fish survival. *Fisheries*
751 *Oceanography*, 5:19–38, 1996.
- 752 Lingyun Nie, Jianchao Li, Hao Wu, Wenchoao Zhang, Yongjun Tian, Yang Liu, Peng Sun, Zhenjiang Ye, Shuyang
753 Ma, and Qinfeng Gao. The influence of ocean processes on fine-scale changes in the yellow sea cold water mass
754 boundary area structure based on acoustic observations. *Remote Sensing*, 15(17):4272, 2023.

- 755 MD Ohman and H-J Hirche. Density-dependent mortality in an oceanic copepod population. *Nature*, 412(6847):
756 638–641, 2001.
- 757 SA Piontkovski, R Williams, and TA Melnik. Spatial heterogeneity, biomass and size structure of plankton of the
758 indian ocean: some general trends. *Marine ecology progress series*, pages 219–227, 1995.
- 759 Emmanuel Potiris, Constantin Frangoulis, Alkiviadis Kalampokis, Manolis Ntoumas, Manos Pettas, George Peti-
760 hakis, and Vassilis Zervakis. Acoustic doppler current profiler observations of migration patterns of zooplankton
761 in the cretan sea. *Ocean Science*, 14(4):783–800, 2018.
- 762 TG Prasad and N Bahulayan. Mixed layer depth and thermocline climatology of the arabian sea and western
763 equatorial indian ocean. 1996.
- 764 SZ Qasim. Biological productivity of the indian ocean. 1977.
- 765 Corinne Le Quéré, Robbie M Andrew, Josep G Canadell, Stephen Sitch, Jan Ivar Korsbakken, Glen P Peters,
766 Andrew C Manning, Thomas A Boden, Pieter P Tans, Richard A Houghton, et al. Global carbon budget 2016.
767 *Earth System Science Data*, 8(2):605–649, 2016.
- 768 Seshagiri Raghukumar and AC Anil. Marine biodiversity and ecosystem functioning: A perspective. *Current Science*,
769 84(7):884–892, 2003.
- 770 CP Ramamirtham and AVS Murty. Hydrography of the west coast of india during the pre-monsoon period of the
771 year 1962—part 2: in and offshore waters of the konkan and malabar coasts. *Journal of the Marine Biological
772 Association of India*, 7(1):150–168, 1965.
- 773 S Ramamurthy. Studies on the plankton of the north kanara coast in relation to the pelagic fishery. *Journal of
774 Marine Biological Association of India*, 7(1):127–149, 1965.
- 775 Mehbuba Rehim and Mudassar Imran. Dynamical analysis of a delay model of phytoplankton–zooplankton interac-
776 tion. *Applied Mathematical Modelling*, 36(2):638–647, 2012.
- 777 T. P. Rippeth and J. H. Simpson. Diurnal signals in vertical motions on the hebridean shelf. *Limnology and
778 Oceanography*, 43:1690–1696, 1998. doi: 10.4319/lo.1998.43.7.1690.
- 779 John H Ryther, John R Hall, Allan K Pease, Andrew Bakun, and Mark M Jones. Primary organic production in
780 relation to the chemistry and hydrography of the western indian ocean 1. *Limnology and Oceanography*, 11(3):
781 371–380, 1966.
- 782 Henrike Schmidt, Rena Czeschel, and Martin Visbeck. Seasonal variability of the arabian sea intermediate circulation
783 and its impact on seasonal changes of the upper oxygen minimum zone. *Ocean Science*, 16(6):1459–1474, 2020.
- 784 D Shankar, SSC Shenoi, RK Nayak, PN Vinayachandran, G Nampoothiri, AM Almeida, GS Michael, MR Ramesh
785 Kumar, D Sundar, and OP Sreejith. Hydrography of the eastern arabian sea during summer monsoon 2002.
786 *Journal of earth system science*, 114:459–474, 2005.

- 787 D Shankar, R Remya, PN Vinayachandran, Abhisek Chatterjee, and Ambica Behera. Inhibition of mixed-layer
788 deepening during winter in the northeastern arabian sea by the west india coastal current. *Climate Dynamics*,
789 47:1049–1072, 2016.
- 790 D Shankar, R Remya, AC Anil, and V Vijith. Role of physical processes in determining the nature of fisheries in the
791 eastern arabian sea. *Progress in Oceanography*, 172:124–158, 2019.
- 792 SSC Shenoi, D Shankar, GS Michael, J Kurian, KK Varma, MR Ramesh Kumar, AM Almeida, AS Unnikrishnan,
793 W Fernandes, N Barreto, et al. Hydrography and water masses in the southeastern arabian sea during march–june
794 2003. *Journal of earth system science*, 114:475–491, 2005.
- 795 SR Shetye, AD Gouveia, SSC Shenoi, D Sundar, GS Michael, AM Almeida, and K Santanam. Hydrography and
796 circulation off the west coast of india during the southwest monsoon 1987. 1990.
- 797 S.R. Shetye, A.D. Gouveia, S.S.C. Shenoi, G.S. Michael, D. Sundar, A.M. Almeida, and K. Santanam. The coastal
798 current off western india during the northeast monsoon. *Deep Sea Research Part A. Oceanographic Research*
799 Papers, 38(12):1517–1529, 1991. ISSN 0198-0149. doi: [https://doi.org/10.1016/0198-0149\(91\)90087-V](https://doi.org/10.1016/0198-0149(91)90087-V). URL
800 <https://www.sciencedirect.com/science/article/pii/019801499190087V>.
- 801 SR Shetye, AD Gouveia, and SSC Shenoi. Does winter cooling lead to the subsurface salinity minimum off saurashtra,
802 india? *Oceanography of the Indian Ocean*, pages 617–625, 1992.
- 803 Wei Shi and Menghua Wang. Phytoplankton biomass dynamics in the arabian sea from viirs observations. *Journal*
804 *of Marine Systems*, 227:103670, 2022.
- 805 Houssem Smeti, Marc Pagano, Christophe Menkes, Anne Lebourges-Dhaussy, Brian PV Hunt, Valerie Allain, Martine
806 Rodier, Florian De Boissieu, Elodie Kestenare, and Cherif Sammari. Spatial and temporal variability of zooplankton
807 off n ew c aledonia (s outhwestern p acific) from acoustics and net measurements. *Journal of Geophysical*
808 *Research: Oceans*, 120(4):2676–2700, 2015.
- 809 Sharon Smith, Michael Roman, Irina Prusova, Karen Wishner, Marcia Gowing, LA Codispoti, Richard Barber, John
810 Marra, and Charles Flagg. Seasonal response of zooplankton to monsoonal reversals in the arabian sea. *Deep Sea*
811 *Research Part II: Topical Studies in Oceanography*, 45(10-11):2369–2403, 1998.
- 812 SL Smith and M Madhupratap. Mesozooplankton of the arabian sea: patterns influenced by seasons, upwelling, and
813 oxygen concentrations. *Progress in Oceanography*, 65(2-4):214–239, 2005.
- 814 Patnaik Sreenivas, KVKRK Patnaik, and KVSR Prasad. Monthly variability of mixed layer over arabian sea using
815 argo data. *Marine Geodesy*, 31(1):17–38, 2008.
- 816 R Subrahmanyam. Studies on the phytoplankton of the west coast of india: Part ii. physical and chemical factors
817 influencing the production of phytoplankton, with remarks on the cycle of nutrients and on the relationship of
818 the phosphate-content to fish landings. In *Proceedings/Indian Academy of Sciences*, volume 50, pages 189–252.
819 Springer, 1959.

- 820 R Subrahmanyam and AH Sarma. Studies on the phytoplankton of the west coast of india. part iii. seasonal variation
821 of the phytoplankters and environmental factors. *Indian Journal of Fisheries*, 7(2):307–336, 1960.
- 822 Laura Ursella, Vanessa Cardin, Mirna Batistić, Rade Garić, and Miroslav Gačić. Evidence of zooplankton vertical
823 migration from continuous southern adriatic buoy current-meter records. *Progress in oceanography*, 167:78–96,
824 2018.
- 825 Laura Ursella, Sara Pensieri, Enric Pallàs-Sanz, Sharon Z Herzka, Roberto Bozzano, Miguel Tenreiro, Vanessa Cardin,
826 Julio Candela, and Julio Sheinbaum. Diel, lunar and seasonal vertical migration in the deep western gulf of mexico
827 evidenced from a long-term data series of acoustic backscatter. *Progress in Oceanography*, 195:102562, 2021.
- 828 V Vijith, PN Vinayachandran, V Thushara, P Amol, D Shankar, and AC Anil. Consequences of inhibition of mixed-
829 layer deepening by the west india coastal current for winter phytoplankton bloom in the northeastern arabian sea.
830 *Journal of Geophysical Research: Oceans*, 121(9):6583–6603, 2016.
- 831 V Vijith, SR Shetye, AD Gouveia, SSC Shenoi, GS Michael, and D Sundar. Circulation in the region of the west
832 india coastal current in march 1994 hydrographic and altimeter data. *Journal of Earth System Science*, 131(1):
833 16, 2022.
- 834 Ian P Wade and Karen J Heywood. Acoustic backscatter observations of zooplankton abundance and behaviour
835 and the influence of oceanic fronts in the northeast atlantic. *Deep Sea Research Part II: Topical Studies in
836 Oceanography*, 48(4-5):899–924, 2001.
- 837 Peter H Wiebe, Charles H Greene, Timothy K Stanton, and Janusz Burczynski. Sound scattering by live zooplankton
838 and micronekton: empirical studies with a dual-beam acoustical system. *The Journal of the Acoustical Society of
839 America*, 88(5):2346–2360, 1990.
- 840 Jerry D Wiggert, RR Hood, Karl Banse, and JC Kindle. Monsoon-driven biogeochemical processes in the arabian
841 sea. *Progress in Oceanography*, 65(2-4):176–213, 2005.
- 842 Monika Winder and Daniel E Schindler. Climatic effects on the phenology of lake processes. *Global change biology*,
843 10(11):1844–1856, 2004.
- 844 Karen F Wishner, Marcia M Gowing, and Celia Gelfman. Mesozooplankton biomass in the upper 1000 m in the
845 arabian sea: overall seasonal and geographic patterns, and relationship to oxygen gradients. *Deep Sea Research
846 Part II: Topical Studies in Oceanography*, 45(10-11):2405–2432, 1998.

Table 1: ADCP deployment details at the locations. The temporal resolution is 1 hour, bin size(vertical resolution) 4 m. All ADCPs are operated at 153.3 kHz. The moorings are at a water column depth of 950–1200 m on the continental slope and are serviced on yearly basis according to ship availability. The 6th column consists of Reference echo intensity (Er) for each beam, while the 7th column contains the corresponding RSSI conversion factor [Deines, 1999].

Station (Position; °E, °N)	Date		Depth			
	Deployment	Recovery	Ocean	ADCP	Er	Kc
Okha (67.47, 22.26)	01/10/2018	01/12/2019	996	118	37 , 37 , 37 , 36	0.42 , 0.44 , 0.42 , 0.43
	01/12/2019	04/12/2020	1166	312	39 , 36 , 38 , 36	0.42 , 0.44 , 0.42 , 0.43
	04/12/2020	08/03/2022	1021	144	41 , 37 , 38 , 37	0.42 , 0.44 , 0.42 , 0.43
	08/03/2022	01/01/2023	1019	142	37 , 38 , 39 , 36	0.42 , 0.44 , 0.42 , 0.43
Mumbai (69.24, 20.01)	09/11/2017	29/09/2018	1025	150	36 , 34 , 39 , 42	0.40 , 0.40 , 0.40 , 0.40
	29/09/2018	29/11/2019	1122	125	35 , 36 , 39 , 42	0.40 , 0.40 , 0.40 , 0.40
	29/11/2019	02/12/2020	1143	164	37 , 34 , 39 , 43	0.40 , 0.40 , 0.40 , 0.40
	02/12/2020	06/03/2022	1125	142	36 , 34 , 39 , 42	0.40 , 0.40 , 0.40 , 0.40
	07/03/2022	02/01/2023	1103	158	37 , 34 , 40 , 43	0.40 , 0.40 , 0.40 , 0.40
Jaigarh (71.12, 17.53)	27/10/2017	27/09/2018	1039	198	32 , 35 , 33 , 32	0.45 , 0.45 , 0.45 , 0.45
	27/09/2018	30/10/2019	1032	164	32 , 35 , 33 , 31	0.45 , 0.45 , 0.45 , 0.45
	03/11/2019	30/11/2020	1142	264	32 , 36 , 33 , 32	0.45 , 0.45 , 0.45 , 0.45
	30/11/2020	05/03/2022	1099	119	33 , 36 , 34 , 32	0.45 , 0.45 , 0.45 , 0.45
Goa (72.74, 15.17)	03/10/2017	25/09/2018	1000	174	35 , 37 , 34 , 35	0.44 , 0.44 , 0.40 , 0.41
	25/09/2018	16/10/2019	969	145	38 , 36 , 36 , 34	0.44 , 0.44 , 0.40 , 0.41
	16/10/2019	29/11/2020	966	143	44 , 38 , 36 , 43	0.44 , 0.44 , 0.40 , 0.41
	29/11/2020	03/03/2022	985	157	35 , 40 , 35 , 38	0.44 , 0.44 , 0.40 , 0.41
	03/03/2022	05/01/2023	984	159	35 , 38 , 35 , 34	0.44 , 0.44 , 0.40 , 0.41
Udupi (74.04, 12.5)	05/10/2017	06/10/2018	1028	176	44 , 46 , 29 , 35	0.45 , 0.45 , 0.45 , 0.45
	06/10/2018	18/10/2019	1027	179	32 , 38 , 30 , 36	0.45 , 0.45 , 0.45 , 0.45
	18/10/2019	11/12/2020	1018	168	33 , 37 , 31 , 38	0.45 , 0.45 , 0.45 , 0.45
	11/03/2022	06/01/2023	1036	155	31 , 32 , 32 , 33	0.45 , 0.45 , 0.45 , 0.45
Kollam (75.44, 9.05)	07/10/2017	08/10/2018	1174	200	43 , 55 , 45 , 43	0.49 , 0.50 , 0.49 , 0.50
	08/10/2018	20/10/2019	1160	123	49 , 62 , 46 , 46	0.49 , 0.50 , 0.49 , 0.50
	20/10/2019	13/12/2020	1209	176	52 , 61 , 54 , 55	0.49 , 0.50 , 0.49 , 0.50
	13/12/2020	13/03/2022	1129	91	49 , 51 , 46 , 47	0.49 , 0.50 , 0.49 , 0.50
	13/03/2022	08/01/2023	1149	164	41 , 48 , 43 , 41	0.49 , 0.50 , 0.49 , 0.50
Kanyakumari (77.39, 6.96)	16/11/2016	08/10/2017	1096	252	37 , 36 , 37 , 37	0.42 , 0.44 , 0.42 , 0.43
	08/10/2017	10/10/2018	1055	181	32 , 34 , 38 , 35	0.45 , 0.45 , 0.45 , 0.45
	10/10/2018	22/10/2019	1075	180	36 , 34 , 39 , 36	0.45 , 0.45 , 0.45 , 0.45
	22/10/2019	14/12/2020	1060	167	33 , 35 , 36 , 35	0.45 , 0.45 , 0.45 , 0.45
	14/12/2020	14/03/2022	1184	287	34 , 36 , 36 , 35	0.45 , 0.45 , 0.45 , 0.45

Table 2:

Volumetric samples of zooplankton of various stations. The sampling depth range is standardised for later years for bin range of 0–25m, 25–50m, 50–75m, 75–100m, 100–150m. The abbreviations are in the following manner: Okha (O), Mumbai (M), Jaigarh (J), Goa (G), Udupi (U), Kollam (K), Kanyakumari (KK); The number tags corresponds to particular cruise of a station.

Sample number	Tag	Lat($^{\circ}$ N)	Lon($^{\circ}$ E)	Date	Time (IST)	Sampling depth range (m)
1-3	G1	15.18	72.79	25 Sep 18	452	50–25, 100–50, 150–100
4-6	G2	15.16	72.71	25 Sep 18	2108	50–25, 100–50, 150–100
7-10	G2	15.16	72.71	25 Sep 18	2137	40–20, 60–40, 80–60, 100–80
11-14	J1			26 Sep 18	2000	40–20, 60–40, 80–60, 100–80
15-17	J2			27 Sep 18	2000	50–25, 100–50, 150–100
18-21	J2			27 Sep 18	2100	40–20, 60–40, 80–60, 100–80
22-25	M1	20	69.19	28 Sep 18	2135	40–20, 60–40, 80–60, 100–80
26-27	M1	20	69.19	28 Sep 18	2205	50–25, 100–50
28-29	M2	20.01	69.2	29 Sep 18	2035	50–25, 100–50
30-33	M2	20.01	69.2	29 Sep 18	2057	40–20, 60–40, 80–60, 100–80
34-37	U1			5 Oct 18	2000	40–20, 60–40, 80–60, 100–80
38-40	U1			5 Oct 18	2100	50–25, 100–50, 150–100
41-43	U2			6 Oct 18	2000	50–25, 100–50, 150–100
44-47	U2			6 Oct 18	2100	40–20, 60–40, 80–60, 100–80
48-51	K1	9.06	75.42	8 Oct 18	421	40–20, 60–40, 80–60, 100–80
52-54	K1	9.06	75.42	8 Oct 18	449	50–25, 100–50, 150–100
55-56	K2	9.04	75.4	8 Oct 18	2027	50–25, 100–50
57-60	K2	9.04	75.4	8 Oct 18	2045	40–20, 60–40, 80–60, 100–80
61-64	G2	15.16	72.74	16 Oct 19	829	50–25, 75–50, 100–75, 150–100
65-67	G3	15.16	72.74	16 Oct 19	1812	50–25, 75–50, 100–75
68-70	K2	9.02	75.42	20 Oct 19	840	50–25, 75–50, 100–75
71-74	K3	9.04	75.43	20 Oct 19	1934	50–25, 75–50, 100–75, 150–100
75-78	KK1			22 Oct 19	742	50–25, 75–50, 100–75, 150–100
79-82	KK2			22 Oct 19	1925	50–25, 75–50, 100–75, 150–100
83-86	J1			30 Oct 19	324	50–25, 75–50, 100–75, 150–100
87-89	J2			4 Nov 19	946	75–50, 100–75, 150–100
90-92	M2	19.98	69.22	29 Nov 19	1434	50–25, 75–50, 100–75
93-96	M3	20.01	69.23	30 Nov 19	958	50–25, 75–50, 100–75, 150–100
97-100	O1	22.24	67.49	1 Dec 19	937	50–25, 75–50, 100–75, 150–100
101	O2	22.25	67.46	1 Dec 19	1957	150–100
102-105	G3	15.68	73.22	28 Nov 20	930	50–25, 75–50, 100–75, 150–100
105-108	G4	15.32	73.22	29 Nov 20	1558	50–25, 75–50, 100–75, 150–100
108-110	J2	17.85	71.21	30 Nov 20	1458	75–50, 100–75, 150–100
111-114	J3	17.91	71.21	1 Dec 20	1052	50–25, 75–50, 100–75, 150–100
115-118	M4	20.03	69.38	2 Dec 20	2016	50–25, 75–50, 100–75, 150–100
119-00	O2	22.41	67.8	4 Dec 20	953	150–100
120-123	O3	22.41	67.79	4 Dec 20	2011	50–25, 75–50, 100–75, 150–100
124-127	K3	9.11	75.72	12 Dec 20	2335	50–25, 75–50, 100–75, 150–100
128-131	K4	9.06	75.74	13 Dec 20	1507	50–25, 75–50, 100–75, 150–100
132-134	KK1	7.62	77.63	14 Dec 20	1226	50–25, 75–50
135-138	KK2	7.62	77.63	14 Dec 20	2047	50–25, 75–50, 100–75, 150–100
139-142	G4	15.32	73.21	3 Mar 22	823	50–25, 75–50, 100–75, 150–100
143-146	G5	15.68	73.21	4 Mar 22	1030	50–25, 75–50, 100–75, 150–100
147-150	M5	19.99	69.23	7 Mar 22	957	50–25, 75–50, 100–75, 150–100
151-154	O3	22.24	67.5	8 Mar 22	806	50–25, 75–50, 100–75, 150–100
155-158	U3	12.5	74.04	12 Mar 22	1156	50–25, 75–50, 100–75, 150–100
159-160	K4	9.04	75.42	13 Mar 22	1027	50–25, 75–50, 100–75
161-164	KK3	6.97	77.4	15 Mar 22	1220	50–25, 75–50, 100–75, 150–100

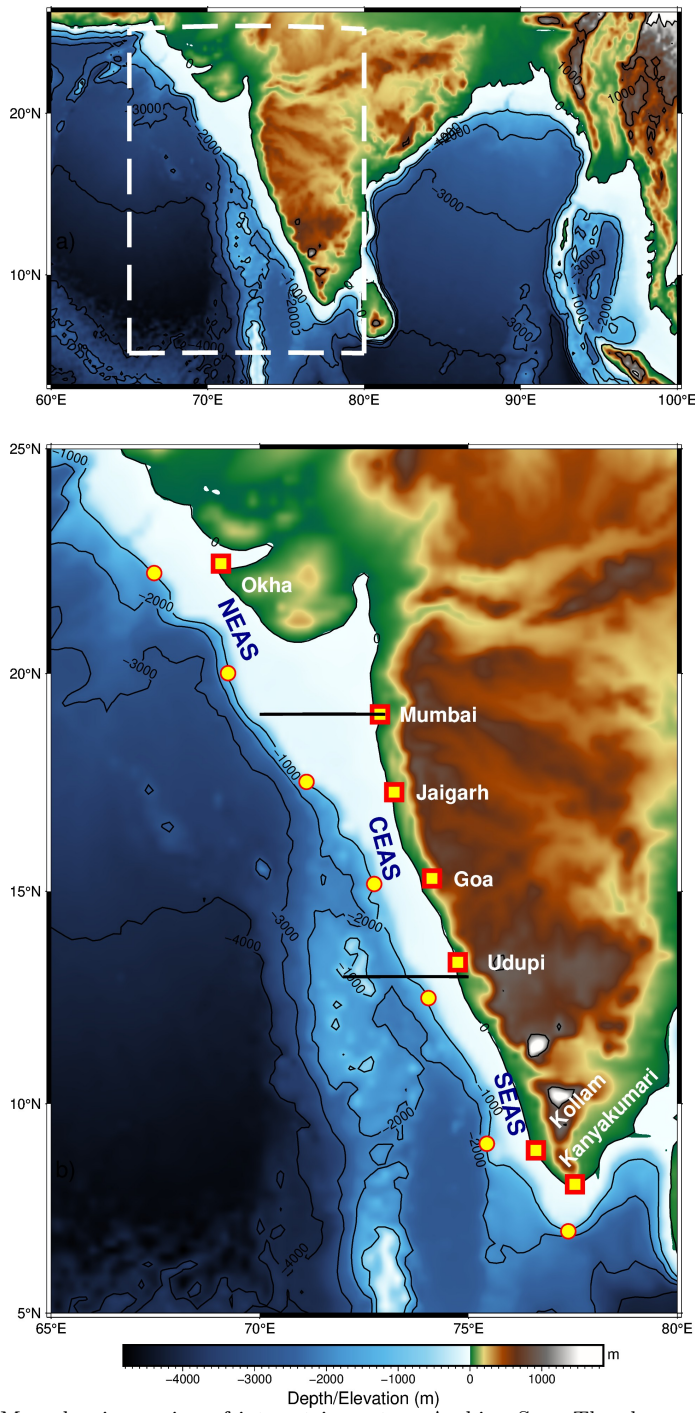


Figure 1: Map showing region of interest in eastern Arabian Sea. The slope moorings are deployed at ~ 1000 m depth as shown in the bathymetry contour. Note the increase in shelf width as we go poleward along the coast. The mooring sites off Okha and Mumbai are in Northern EAS; Jaigarh and Goa in Central EAS while Kollam and Kanyakumari are at Southern EAS. Udupi is situated at the transition zone of Central and Southern EAS.

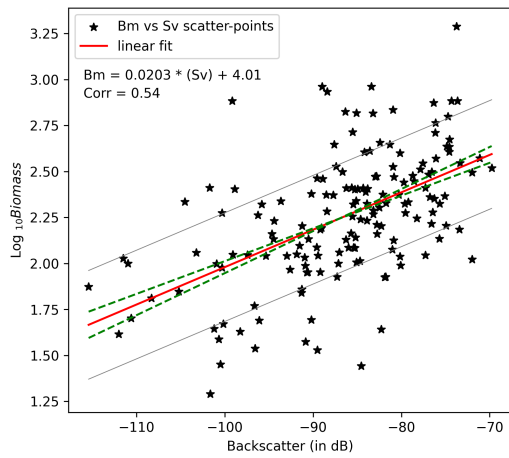


Figure 2: The linear fit line of Biomass (\log_{10} scale) and backscattering strength (in dB). The linear fit line is within the error range of previous result of [Aparna et al., 2022] (contained 67 data points) onto which latest zooplankton volumetric sample data (159 data points) is appended. The regression equation is $y = (0.02 \pm 0.0025) x + (4.0144 \pm 0.2198)$ and correlation value of 0.54. The dashed green lines denote error range of plausible slope and intercept. From the linear equation, the upper and lower bound of error limit leads to an error bar of $\sim 14 \text{ mg m}^{-3}$. Standard deviation σ of $\log_{10}(\text{Biomass})$ is ± 0.49 , which results in the backscatter range of 48.58 dB encompassing the entire backscatter range. It signifies the robustness of zooplankton biomass dependency on ADCP measured backscattering strength.

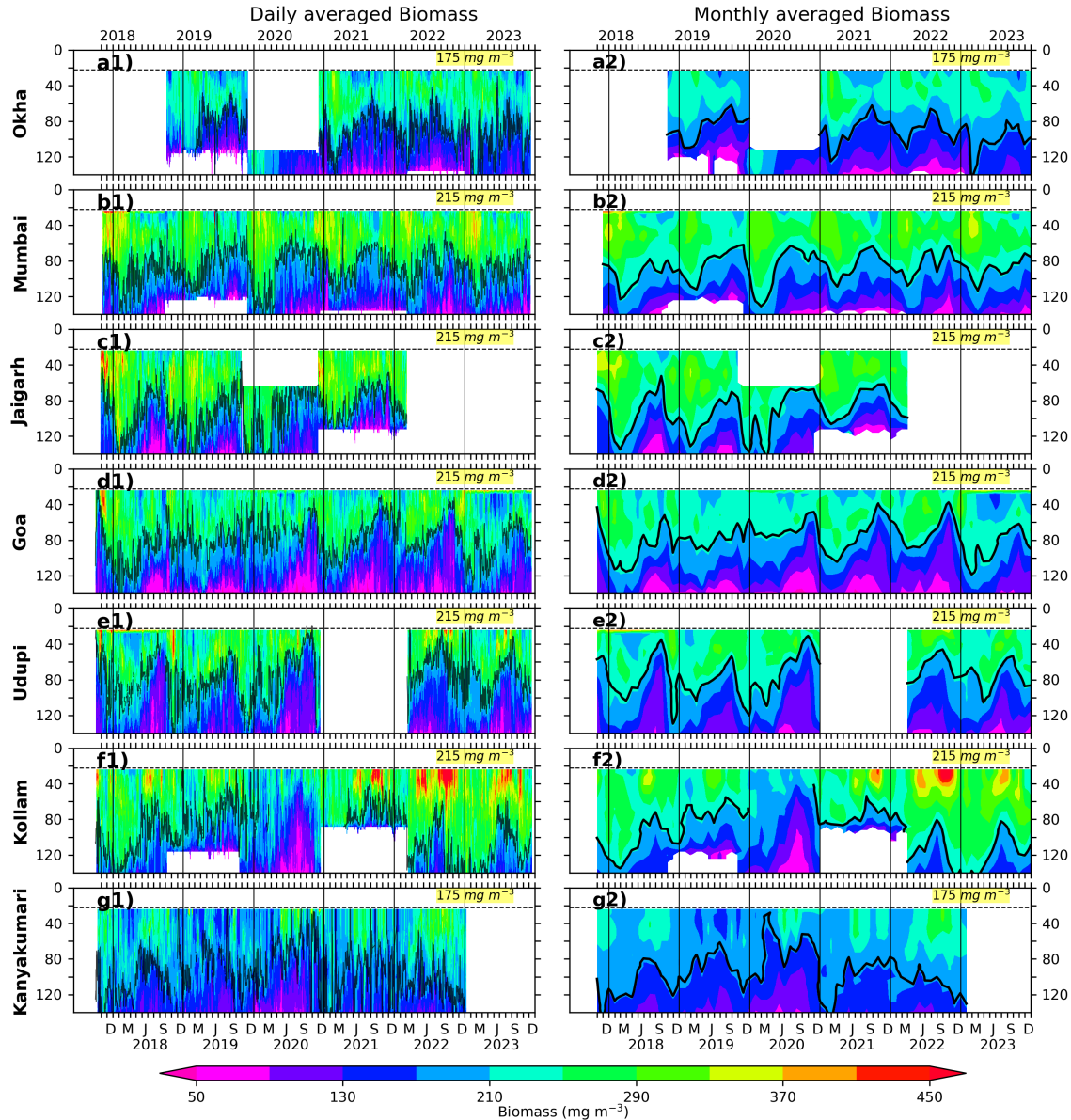


Figure 3: The Daily and monthly averaged biomass for EAS moorings, north (top) to south (bottom). The black contours are marking of 175 mg m^{-3} biomass for Okha and Kanyakumari; 215 mg m^{-3} for Mumbai, Goa and Kollam. The biomass contours are distinct and different based on the physico-chemical parameters and the one that best explains seasonality at respective location. The top 10% of data is discarded due to echo noise. The dashed line at 22 m marks the top-depth of first bin i.e, 24 m. During 2020 off Kollam, a lack of suitable biomass contour showing seasonality is due to strong interannual variations.

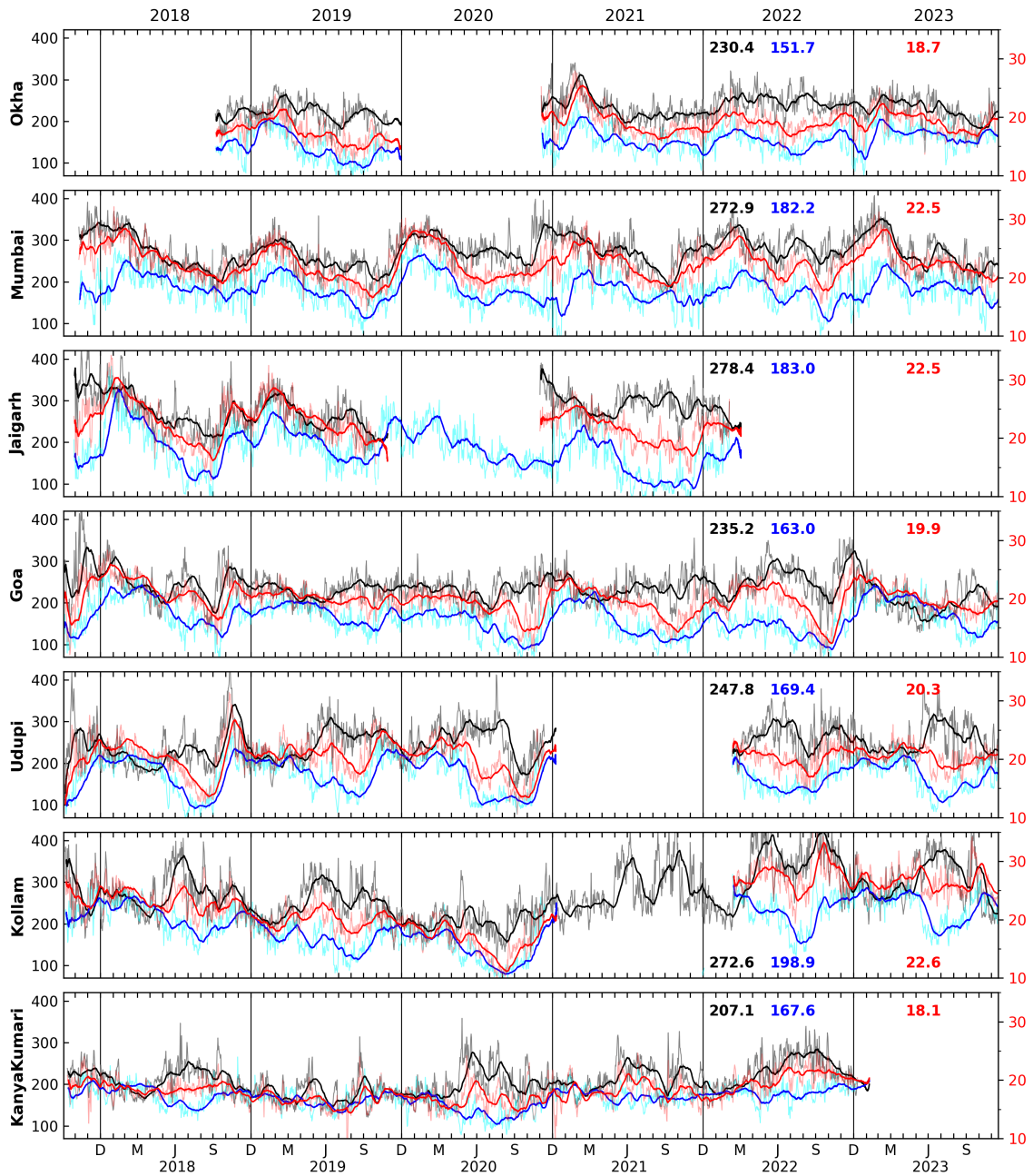


Figure 4: The daily biomass at depth of 40 m and 104 m and ZSS for all locations shown by grey, cyan, and pink curves with the black, blue, and red lines shows the 30 day rolling averaged biomass at 40 & 104 m, and ZSS, respectively. The mean biomass at 40 and 104 and mean ZSS is shown in top right corresponding to those colors. Notice the spikes (bursts) seen in the daily (rolling mean) data of biomass at 40 m that lasts few days (few days to weeks), e.g., during many isolated days of June of 2020 (during entire June–July of 2020). These spikes and bursts are seen at all locations and both at 40 and 104 m, albeit with a varied magnitude.

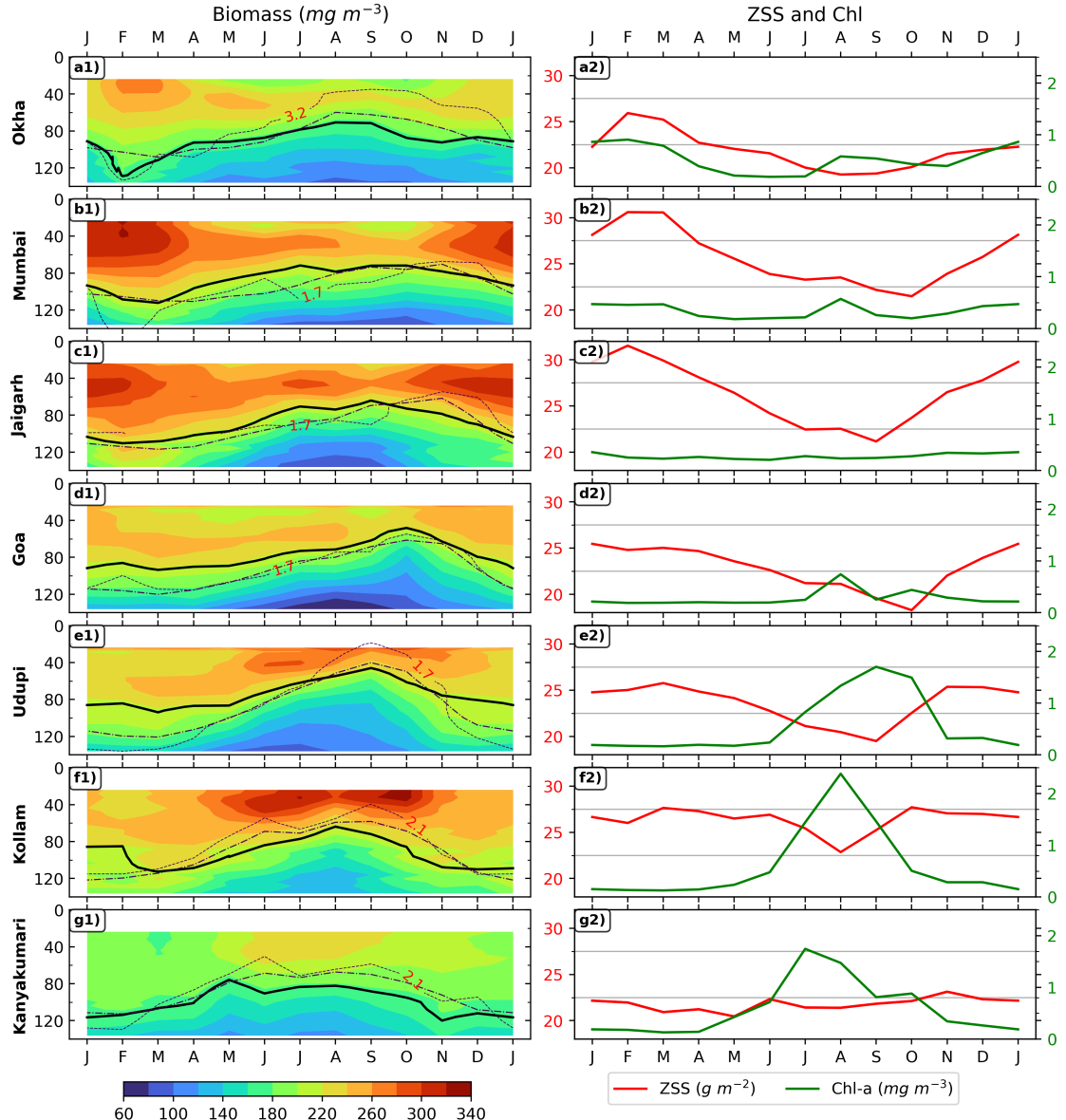


Figure 5: Monthly climatology of zooplankton biomass is shown in left panels for 7 locations, (top to bottom is southward). The D175 and D215 are shown in solid lines; dashed line represents the depth of 23 C isotherm; oxygen contours are shown in dotted lines and labeled for each mooring. The right set of panel plots is showing ZSS (24–140 biomass integral) and chl-a climatology for corresponding locations.

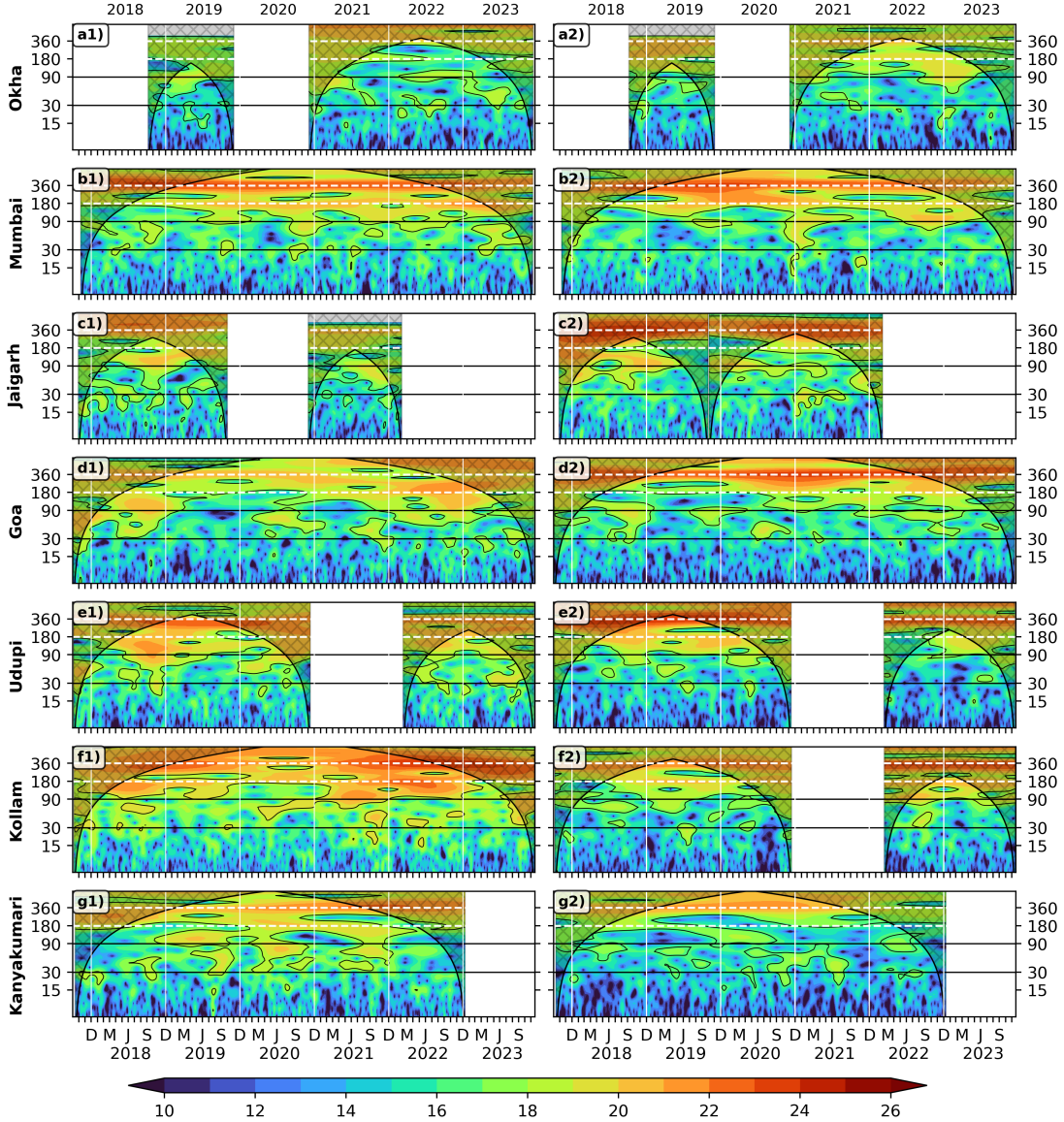


Figure 6: Wavelet power spectra (Morlet) of the 40 m (left panel) and 104 m (right panel) zooplankton biomass plotted against time as abscissa and period in days as ordinate. The wavelet power is in log₂ scale, the 95% significance is marked in black contours; the cross-shaded region falls under cone of influence. The horizontal dashed white (solid black) lines shows annual and semi-annual periods (intraseasonal band). Vertical white lines separates years.

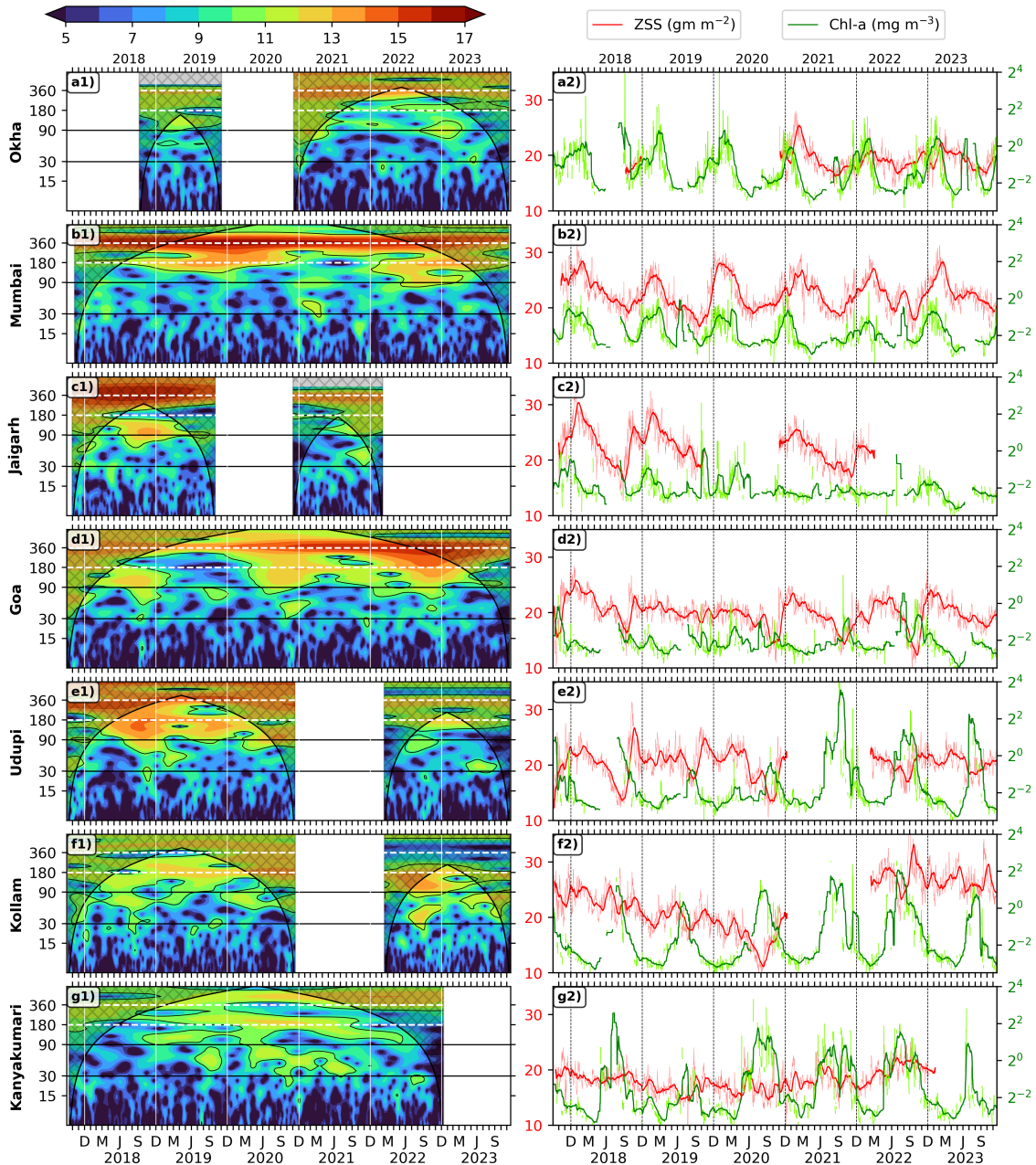


Figure 7: Wavelet power spectra (Morlet) of zooplankton standing stock plotted against time as abscissa and period in days as ordinate. The wavelet power is in \log_2 scale, the 95% significance is marked in black contours; The vertical white lines separates years. The right side panel shows the ZSS (24–120 m biomass integral) time series of 30 day rolling mean data (black) overlaid upon daily data (Grey). The 30 day rolling mean data of chl-a (solid blue) is plotted over its daily data (cyan).

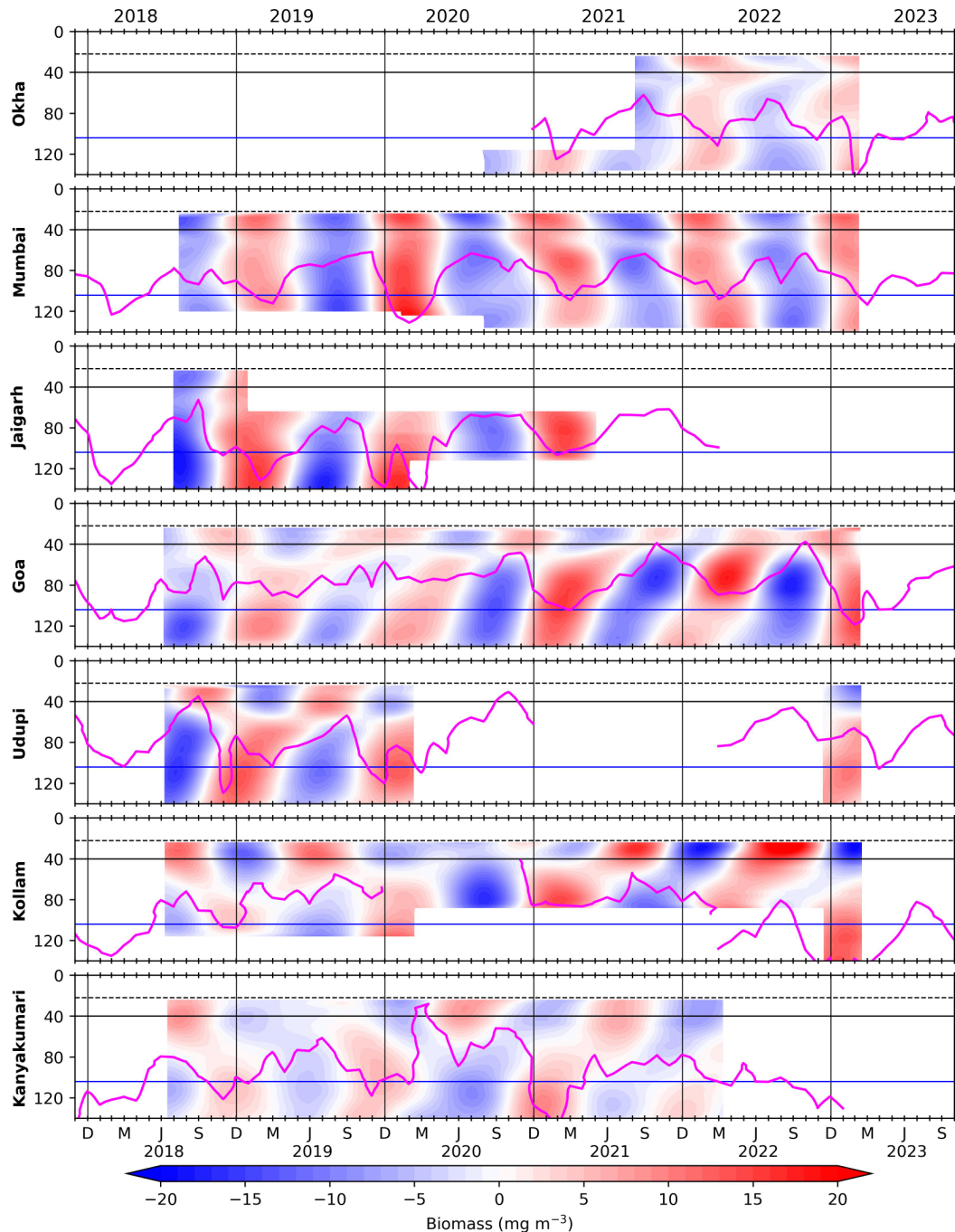


Figure 8: The biomass variation occurring in annual band (300 to 400 days). Owing to the presence of seasonal reversal of current, there is a variation driven by associated upwelling (downwelling) processes in summer (winter) monsoon. The horizontal black and blue lines is for 40 and 104 m, and the standard deviation of biomass at those depths are shown in respective colors at top right corner of each panel; vertical black lines separate the years. The dashed line at 22 m marks the top-depth of first bin i.e, 24 m and solid magenta curves denotes D215 (D175 off Okha and Kanyakumari)

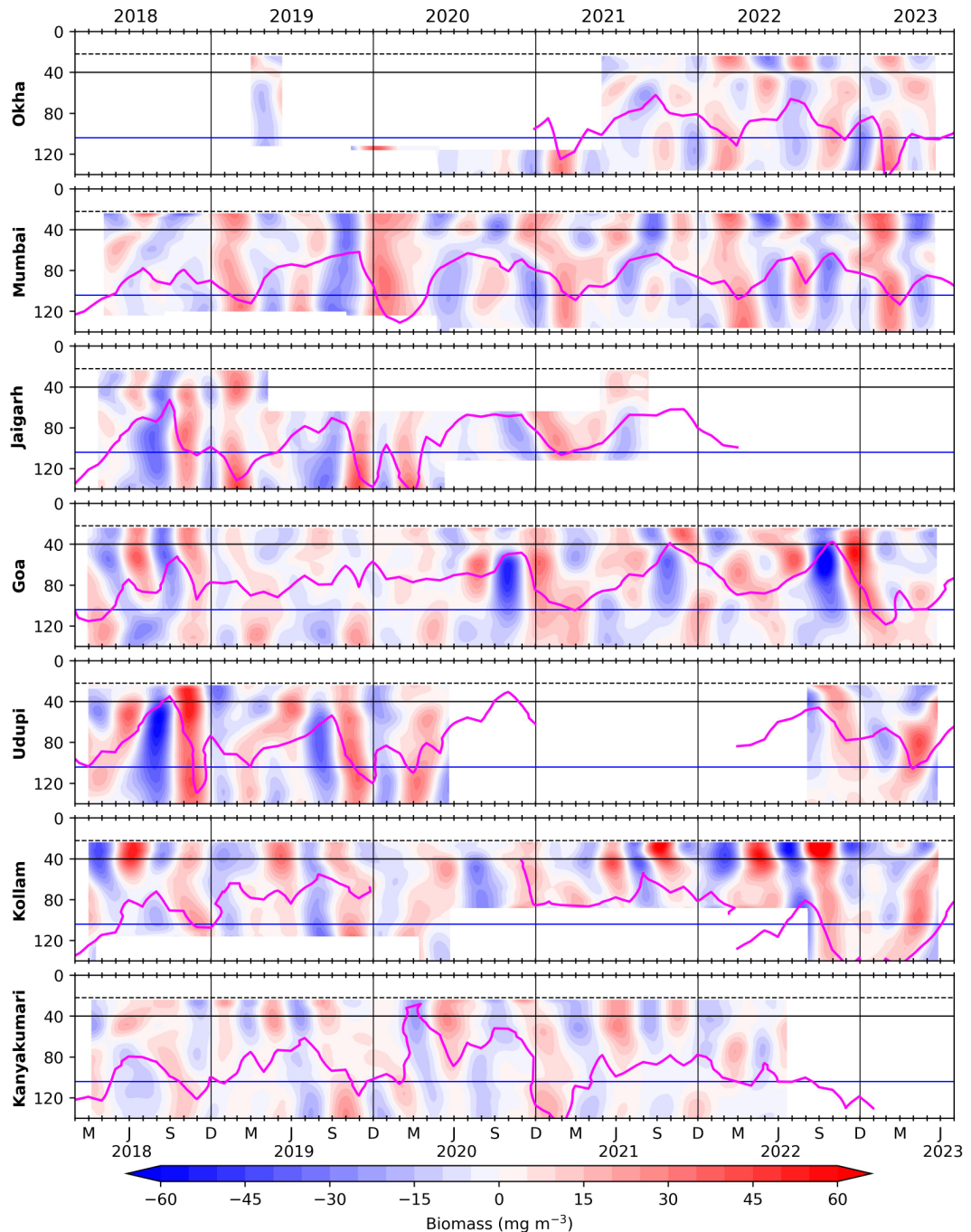


Figure 9: The biomass variation occurring in 100 to 250 days period (between the seasons and within a year record or intra-annual band) is obtained using a band pass filter. The horizontal black and blue lines is for 40 and 104 m, vertical black lines separate the years. The dashed line at 22 m marks the top-depth of first bin i.e, 24 m and solid magenta curves denotes D215 (D175 off Okha and Kanyakumari).

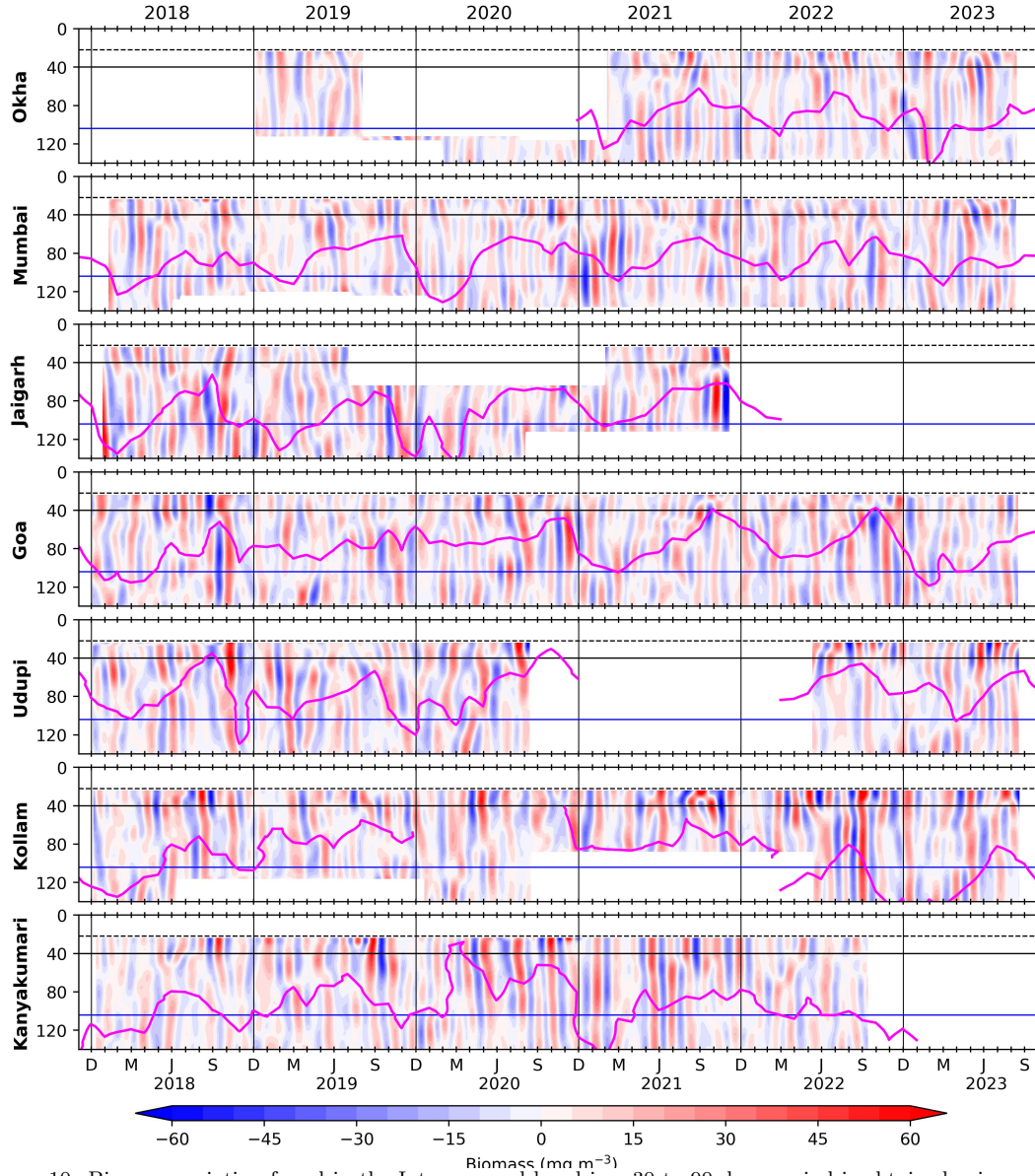


Figure 10: Biomass variation found in the Intraseasonal band i.e., 30 to 90 days period is obtained using a lanczos band pass filter. The horizontal black and blue lines is for 40 and 104 m; vertical black lines separate the years and solid magenta curves denotes D215 (D175 off Okha and Kanyakumari). The dashed line at 22 m marks the top-depth of first bin i.e, 24 m. Intraseasonal variability is seen throughout the record, is coherent along the slope and its magnitude is stronger during August to November.

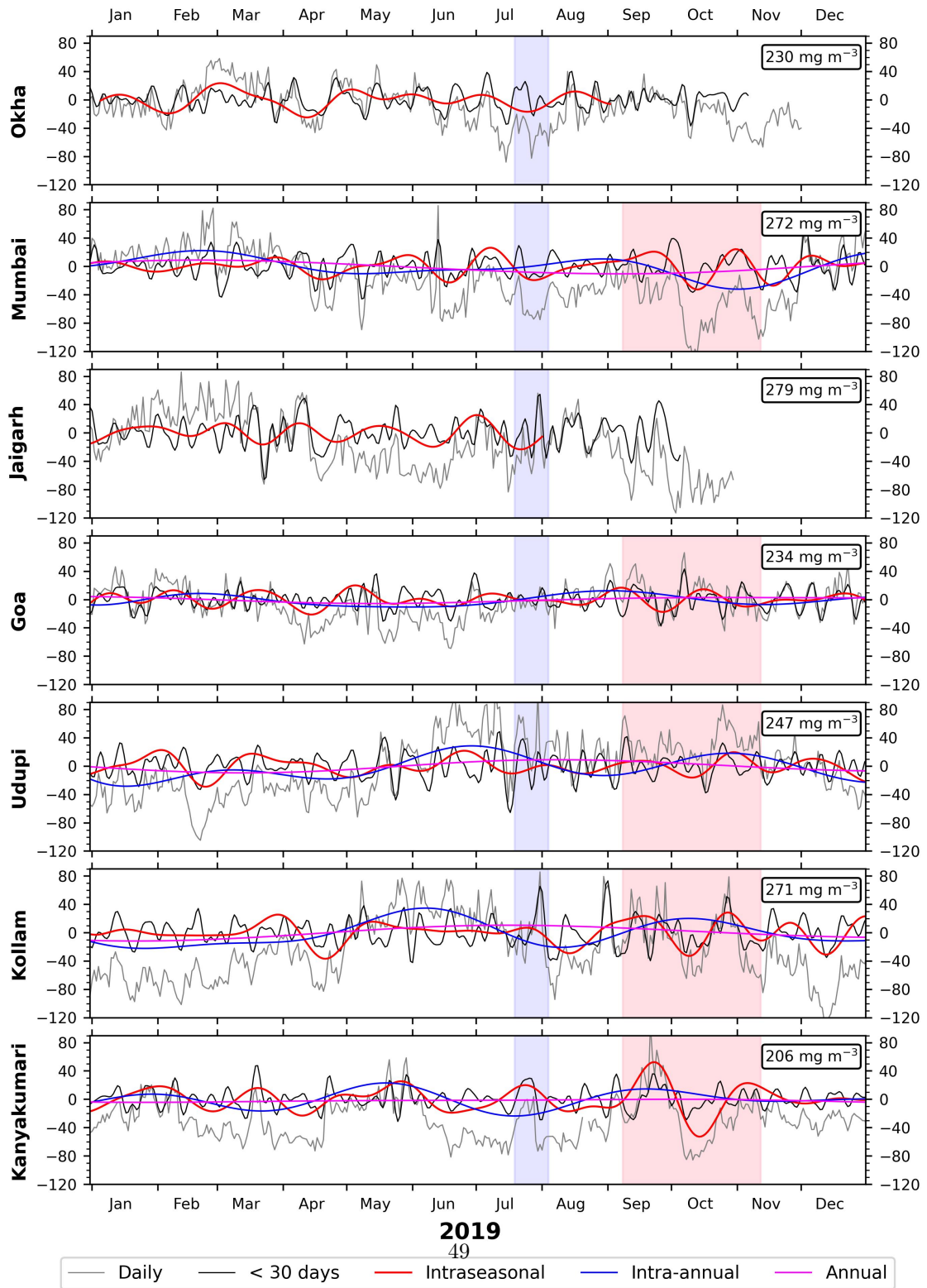


Figure 11: Comparison between mean-removed daily biomass time series at 40 m and the distinct components of variability off Mumbai, Goa and Kollam for 2019. The biomass units are mg m^{-3} and its mean for respective location is shown in top right box. Off Mumbai and Kollam, an increase in biomass is noticed from May onward and lasting till late monsoon with weeks of low biomass during August due to low contribution of intraseasonal component of variability. The pink (green) highlighted region shows coherence in 30–90 days intraseasonal band (daily data) of 40 m biomass. The standalone spikes are representative of patchiness i.e., dense clusters of zooplankton and may not necessarily be observed elsewhere. The annual variability is very weak and lies close to zero almost always.